frontiers | Frontiers in Marine Science

TYPE Original Research
PUBLISHED 24 October 2024
DOI 10.3389/fmars.2024.1434007



OPEN ACCESS

EDITED BY
Francisco Machín,
University of Las Palmas de Gran Canaria, Spain

REVIEWED BY
Ivan Pérez-Santos,
University of Los Lagos, Chile
Catharina Alves-de-Souza,
University of Concepcion, Chile

*CORRESPONDENCE
Barbara Gianella Jacob
barbara.jacob@ciep.cl

RECEIVED 17 May 2024
ACCEPTED 05 September 2024
PUBLISHED 24 October 2024

CITATION
Jacob BG, Astudillo O, Dewitte B, Valladares M, Alvarez Vergara G, Medel C, Crawford DW, Uribe E and Yanicelli B (2024) Abundance and diversity of diatoms and dinoflagellates in an embayment off Central Chile (30°S): evidence of an optimal environmental window driven by low and high frequency winds.
*Front. Mar. Sci.* 11:1434007.
doi: 10.3389/fmars.2024.1434007



# Abundance and diversity of diatoms and dinoflagellates in an embayment off Central Chile (30°S): evidence of an optimal environmental window driven by low and high frequency winds

Barbara Gianella Jacob[1,2*], Orlando Astudillo[2,3], Boris Dewitte[2,3,4], María Valladares[5,6,7], Gonzalo Alvarez Vergara[3], Carolina Medel[8], David W. Crawford[9], Eduardo Uribe[3] and Beatriz Yanicelli[10,11]

[1]Centro de Investigación en Ecosistemas de la Patagonia (CIEP), Coyhaique, Chile, [2]Centro de Estudios Avanzados en Zonas Áridas (CEAZA), Coquimbo, Chile, [3]Facultad de Ciencias del Mar, Departamento de Ciencias del Mar, Universidad Católica del Norte, Coquimbo, Chile, [4]CECI, Université de Toulouse, CERFACS, CNRS, Toulouse, France, [5]Instituto de Políticas Públicas, Universidad Católica del Norte, Coquimbo, Chile, [6]Coastal Solutions Fellows Program, Cornell Lab of Ornithology, Ithaca, NY, United States, [7]Instituto de Ecología y Biodiversidad (IEB), Santiago, Chile, [8]Instituto de Fomento Pesquero (IFOP), CTPA-Putemún, Chiloé, Chile, [9]Independent Researcher, Southampton, United Kingdom, [10]Departamento Interdisciplinario en Sistemas Costeros y Marinos, Centro Universitario Regional Este, Universidad de la República, Rocha, Uruguay, [11]Facultad de Ecología y Manejo Sustentable de Islas Oceánicas, Departamento de Biología Marina, Universidad Católica del Norte, Coquimbo, Chile

The relationship between phytoplankton abundances and wind forcing in upwelling systems involves a number of processes that make the relationship nonlinear in nature. In particular, although upwelling-favorable winds tend to provide nutrients for phytoplankton growth, they can also induce export of both biomass and nutrients to the open ocean through Ekman and eddy-induced transport, or dilution of populations through vertical mixing, which negatively impacts increase in biomass. These processes are essentially nonlinear and can interact antagonistically or synergistically on the overall coastal accumulation of biomass. Consequently, producers and consumers tend to decline above a certain wind threshold despite input of nutrient-enriched water. We have observed this phenomenon in an embayment off Central Chile (30°S), where almost 10 years (2000-2009) of microphytoplankton data were analyzed together with environmental variables and wind phenology. Our findings showed that abundance, species diversity and evenness of diatoms and dinoflagellates all increased post-2005 when the mean of the alongshore surface wind stress reached a maximum threshold value of 0.026 N $m^{-2}$, observed at the decadal temporal variability scale. The increased abundances of diatoms and dinoflagellates post-2005 was associated with the changing phase of the Pacific Decadal Oscillation (PDO) from positive (warm) to negative (cold) phases, which was also associated with a decrease in the intra-seasonal wind activity. Both abundance and diversity of the microphytoplankton community peaked during the post-2005 period whereas higher abundances and frequency of harmful algal blooms (e.g. *Pseudo-nitzschia australis*) were

observed prior to 2005. We suggest that the low-frequency (decadal) variations of mean wind stress during a transition phase of the PDO combined with the reduction in intra-seasonal (periods shorter than 2 months) wind variability after 2005 provided an "optimal environmental window" for the ecosystem.

KEYWORDS

**wind phenology, pacific decadal oscillation, microphytoplankton abundance and diversity, upwelling system, optimal environmental window, harmful algal blooms**

# 1 Introduction

Marine phytoplankton play pivotal roles in primary production, global oceanic biogeochemical cycles, ecosystem stability, human food security, and climate regulation (Falkowski et al., 1998, 2008; Khatiwala et al., 2009; Falkowski, 2012; Blanchard et al., 2012; Toseland et al., 2013). Diatoms are one of the most important prominent microphytoplankton groups, with more than 12000 species (Mann and Vanormelingen, 2013) distributed ubiquitously in marine environments worldwide. They play many functional roles, contributing to ~40% of primary production (Field et al., 1998), and play a major role in the carbon cycle and the biogeochemical cycling of nutrients, such as nitrogen and silicon (reviewed by Benoiston et al., 2017). Dinoflagellates represent a second important group of microphytoplankton that includes more than 2300 species distributed in marine waters worldwide (Lundholm and Moestrup, 2006; Gomez, 2012a), with a diverse range lifestyles (e.g., free-living, parasitic, mutualistic) and trophic modes (e.g., autotrophic, mixotrophic, and heterotrophic) (Gomez, 2012b; Flynn et al., 2019). Photosynthetic and free-living dinoflagellates constitute a part of the ocean food web and contribute to primary production and cycling of organic carbon and nitrogen (Ishida et al., 2023). Dinoflagellates also produce toxic or noxious harmful algal blooms (HABs), which have negative impacts on human health, socioeconomic activities, and ecosystems (Brown et al., 2020; Grattan et al., 2016; Díaz and Alvarez, 2023; Díaz et al., 2023).

Marine phytoplankton exhibit pronounced spatiotemporal dynamics, with recurring seasonal phenological patterns (Nohe et al., 2020). On a global scale, traditional phytoplankton studies and models of ocean chemistry and biology have predicted that primary production will decline as the ocean surface warms and becomes increasingly stratified. This could lead to a shallower mixed-layer and a disconnection between wind stress and coastal upwelling below 100 m depth (Boyce et al., 2010; Fu et al., 2016; Osman et al., 2019; Oyarzun and Brierley., 2018) which, combined with ocean acidification and deoxygenation, is likely to force a reorganization of phytoplankton communities (Henson et al., 2021). Global change threatens ecosystem functioning by reducing opportunities for species coexistence (Matías et al., 2018) which ultimately reduces ecosystem stability (Isbell et al., 2015; McCann, 2000) and ecosystemic services (Henson et al., 2021).

Estimated changes in chlorophyll-a using satellite remote sensing have shown diverse responses to climate change over spatial (e.g. coastal zone vs open ocean) (Gregg et al., 2005; Antoine et al., 2005) and temporal scales (Behrenfeld et al., 2006; Martínez et al., 2009). Over the longer-term, phenological fluctuations in phytoplankton have been shown to be strongly correlated with basin-scale climatic modes (Chiba et al., 2012) whereas declining biomass trends are related to increasing sea surface temperatures (Boyce et al., 2010). Climatic modes affect the mixed-layer structure of individual basins and modulate the fluxes of deep-ocean nutrients to the euphotic layer (Miller et al., 2004; Blanco et al., 2002; Carr et al., 2002). Interannual to decadal changes in global phytoplankton abundances are related to basin-scale oscillations of the physical ocean and the interaction between the main pycnocline and upper ocean seasonal mixed layer (Martinez et al., 2009). Thus, basin-scale ocean dynamic processes such as the El Niño-Southern Oscillation (ENSO) or the Pacific Decadal Oscillation (PDO) connect physical, climate-related variability to changes in local phytoplankton productivity and distribution (Martinez et al., 2009; Chavez et al., 2011; Racault et al., 2017) making the relationship between wind and lower trophic levels generally highly nonlinear.

In general, the relationship between wind speed and biological productivity has been described as "dome-shaped" (Botsford et al., 2003), peaking at optimal speed and then falling off at higher wind speeds (e.g. Stone et al. (2020). Numerous studies on the relationship between biological productivity and wind patterns in upwelling systems have suggested that moderate wind speeds yield higher productivity on the shelf (Stone et al., 2020; Botsford et al., 2003; García-Reyes et al., 2014). A moderate speed has been assumed as the "optimal wind window" for the recruitment of small pelagic fish (i.e. Peruvian anchoveta and Pacific Sardine) that relies on biological productivity, concentration, and retention of shelf waters (Cury and Roy, 1989). Biological productivity should be triggered by the intermittence between moderate upwelling-favorable winds to bring nutrients to the euphotic zone, followed by a period of wind relaxation, with timescales (synoptic) on the order of phytoplankton blooms (Largier et al., 2006; Botsford et al.,

2003, 2006; Wilkerson et al., 2006). This wind relaxation helps retain the phytoplankton community (e.g diatoms and dinoflagellates) over the shelf, thus allowing ample time for cells to utilize nutrients (Largier et al., 2006; Hickey and Banas, 2008). Whereas lower winds may limit productivity owing to reduced nutrient supply to the euphotic zone, higher wind speeds tend to promote turbulent mixing and offshore transport, resulting in enhanced vertical dilution and stronger light limitation of growth of phytoplankton in the resulting deeper mixed layer (Xue et al., 2022). In other words, while an increase in upwelling favorable winds tends to provide more nutrients for growth, it also enhances offshore export, opposing the accumulation of biomass within near-surface waters (Botsford et al., 2003; Stone et al., 2020). These processes are essentially non-linear (Gruber et al., 2011), and can interact antagonistically or synergistically, and trigger a variety of phytoplankton community responses.

In the coastal upwelling ecosystems of the South Pacific, the Southeast Pacific Subtropical Anticyclone (SPSA) represents the dominant forcing of the subtropical gyre and is responsible for the seasonal pattern of upwelling favorable winds (Montecino et al., 2006). The intensity and position of the SPSA exhibits an interdecadal oscillation capable of modifying large-scale atmospheric circulation with consequences for coastal upwelling systems (Ancapichún and Garcés-Vargas, 2015). The SPSA is in particular stronger during the cool phase of the PDO (Garreaud and Battisti, 1999; Pezza et al., 2007; Ancapichún and Garcés-Vargas, 2015), which intensifies alongshore winds (Schneider et al., 2017). The PDO represents the main source of oceanic interdecadal variability over the area and explains 49% of the decadal variance in the Pacific region (Ancapichun and Garcés-Vargas, 2015). In recent decades (period 2000-2012), the SPSA showed an intensification and shift toward the southwest associated with a change from a positive to a negative phase of the PDO. This shift has been associated with an increase in alongshore wind stress, offshore Ekman transport (cooler condition) and Ekman suction along the coast of central Chile (Ancapichun and Garcés-Vargas, 2015) and has been suggested to be the cause of the observed coastal cooling that was observed from the 2000s at 33°S (central Chile) (Ancapichún and Garces-Vargas, 2015; Aguirre et al., 2018) and 37°S (southern Chile) (Schneider et al., 2017; Aguirre et al., 2018, 2021).

Tongoy Bay at 30°S in the Coquimbo region is located in one of the main upwelling centers and low-level wind speed/stress maxima off central Chile (see Figures 1A, B). Here, upwelling occurs year-round and is more intense during the austral spring-summer seasons (Rahn, 2012; Bravo et al., 2016). This is an equatorward facing bay in north-central Chile bounded to the west by Lengua de Vaca Point, a 6 km-long northward protruding peninsula (Moraga-Opazo et al., 2011). Such a geographical setting is favorable to the phenomena of "upwelling shadows" where offshore upwelled waters off the peninsula are not directly advected to the center of the bay but instead enter it through a cyclonic baroclinic gyre (10-20 km in diameter). Most field studies carried out off northern Chile have addressed seasonal and interannual scales of variability, however

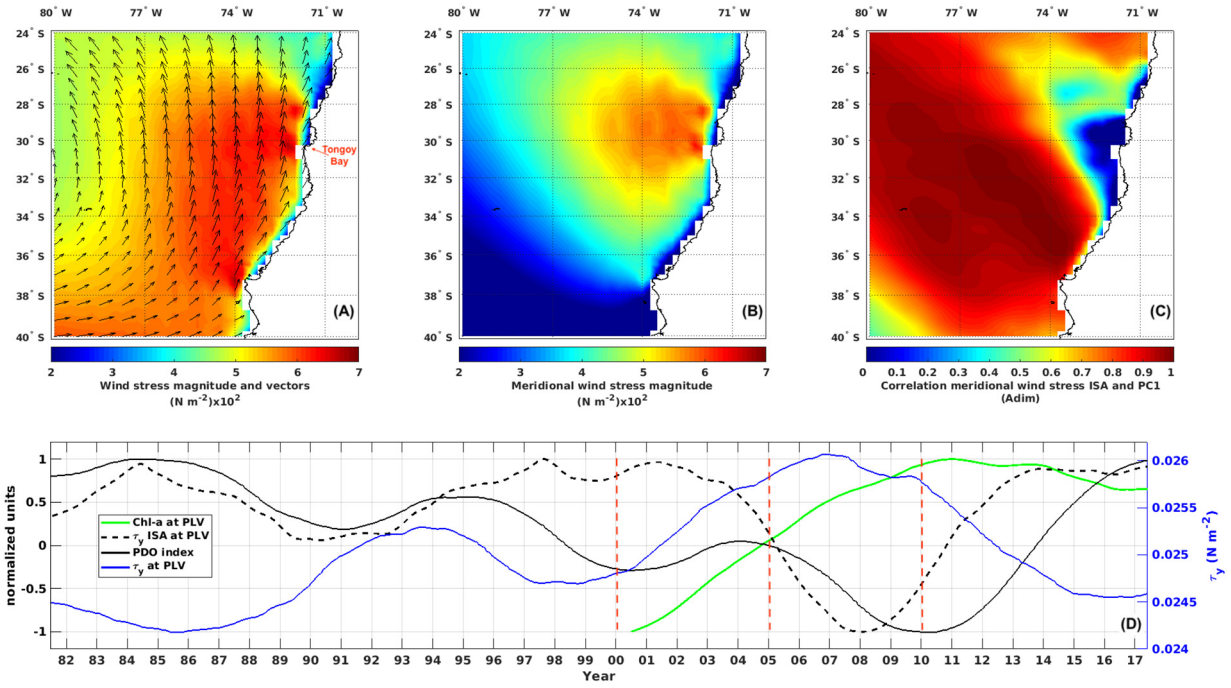


FIGURE 1
Maps of **(A)** ERA5 mean wind stress magnitude (color) and direction (vectors) **(B)** mean meridional wind stress magnitude ($\tau_y$) and **(C)** Pearson correlation between the meridional wind stress Intra-Seasonal Anomalies ($\tau_y$ ISA) and the first principal component (PC1) associated with the dominant variability mode of the $\tau_y$ ISA (60% explained variance) during the period 1982-2017 **(D)** (green line) normalized satellite chlorophyll-a concentration at Punta Lengua de Vaca (PLV), (black continuous line) normalized Pacific Decadal Oscillation (PDO) index, (black dashed line) normalized 3-month running variance of the $\tau_y$ ISA and (blue line) alongshore wind stress ($\tau_y$) at PLV. Note that all of the time series were monthly averaged and filtered with a twice 5-year (61 months) running average. The vertical red dashed lines indicate the periods of interest.

the underlying mechanisms that explain the phenology of the microphytoplankton community at low-frequency (decadal) and high-frequency (intra-seasonal) timescales remain elusive within the Humboldt Current System.

In the present study, we focus on understanding how abundance, composition and biodiversity within diatoms and dinoflagellates – the most important microphytoplankton groups – responded to the alongshore wind stress over a range of timescales of variability (i. e. from intra-seasonal, seasonal to decadal) in Tongoy Bay. Our motivation is to interpret a shift in abundance and diversity of diatoms and dinoflagellates that occurred in 2005 in this bay, and to gain insights into the physical processes controlling changes in coastal community ecology in this upwelling ecosystem in order to increase our capacity to predict future responses to climate change. Our hypothesis was that the observed changes in abundance and diversity during 2000-2009 were driven by PDO-induced shifts in the coastal mean alongshore favorable winds, but that changes in intra-seasonal wind variability are also relevant. More specifically, the sharp increase in community abundances observed since 2005 is suggested to be linked to the shift from the warm phase to the cold phase of the PDO and the concomitant change in high-frequency wind activity on the intra-seasonal scale.

Preserved biological samples were provided by the local aquaculture industry as part of their routine monitoring for harmful algal blooms, where the principal focus is on diatoms and dinoflagellates. Although phototrophic diatoms and dinoflagellates functionally overlap to some extent in terms of physiology (Glibert, 2016), some dinoflagellate genera such as *Dinophysis* can be mixotrophic with others such as *Protoperidinium* being heterotrophic and classified within the microzooplankton (Reviewed by Millette et al., 2023; Mitra and Leles, 2023; Mitra et al., 2023). Microphytoplankton communities are regulated by the interplay between individual species traits, biotic interactions, and the environment, and these interacting challenges hinder the identification of specific trophic roles (Litchman and Christopher, 2008; Elferink et al., 2020). Our total counts include some heterotrophic dinoflagellates and mixotrophic dinoflagellates, but do not include mixotrophic ciliates such as *Mesodinium* and *Laboea* although these genera can contribute significantly to total chl-a and photosynthesis in some marine environments (Stoecker et al., 1987). Despite the focus on diatoms and dinoflagellates, as in other studies (Nohe et al., 2020), it should be emphasized that these are the two principal microphytoplankton groups and are responsible for the bulk of variations in nitrate driven primary production in many marine environments (e.g. Crawford et al., 2018).

The paper is organized as follows. We describe shifts in abundance, diversity and specific composition of the microphytoplankton assemblages in Tongoy Bay during the study period between 2000 and 2009. We focus on seasonal and annual variability of the community of diatoms and dinoflagellates and environmental drivers – before and after 2005 – at intra-seasonal, seasonal and decadal timescales. We also analyzed the upwelling, relaxation and downwelling activity using indices based on daily alongshore wind stress ($\tau_y$) and magnitude, and Sea Surface Temperature (SST) anomalies.

# 2 Materials and methods

## 2.1 Field sampling design

Biological observations from three stations: T4 (30°16′3′′ S - 71°32′07′′ W); T5 (30°17′28′′ S - 71°33′07′′ W) and T11 (30°15′28′′ S - 71°29′50′′ W) positioned throughout Tongoy Bay (north-central Chile, 30°S) were carried out from May 2000 to August 2009 (Figure 2). Hydrographic measurements of temperature and dissolved oxygen (DO) were conducted using a CTD-O at eight stations (St) located in two aquaculture concessions (4 St from the Ostimar S.A and 4 St from San Jose S.A) within Tongoy Bay during the period from January 2001 to August 2008. The monitoring of biological and hydrographic parameters was performed simultaneously during most of the study period, except during the period between May-December 2000 and September 2008-August 2009 where non hydrographic data was available. Hydrographic monitoring and biological samples were carried out fortnightly or weekly which was regulated by the monitoring of the mollusk health program whose objective was to guarantee the food safety of the aquaculture industry. Therefore, sampling frequency shifted from fortnightly to weekly when the marine environment was affected by harmful algal blooms. Thus, a total of 833 surveys of CTD profiles over 92 months (number of surveys per month ranged between 1 and 18; total missing data for 5 months) and a total of 205 surveys of the microphytoplankton community were carried out over a total of 112 months (number of surveys per month ranged between 1 and 6; total missing data 5 months) during the study period (May 2000- August 2009).

## 2.2 Composition, abundance, and diversity of diatoms and dinoflagellates

Water samples for quantitative analyses were collected using a hose sampler that provides an integrated sample between 0 - 10 m, a method recommended by the ICES Working Group on Exceptional Algal Blooms (Lindahl, 1986) to monitor harmful species with heterogeneous vertical distributions. The samples were immediately fixed on board the vessel with acidic Lugol's iodine solution (Lovegrove, 1960). Aliquots (10 or 25 mL) of each sample were placed in Utermöhl chambers for 24 h. Diatom and dinoflagellate species were identified and counted on inverted microscope models Nikon Diaphot (2000 – 2006) and Olympus IX71 (2007 – 2009) using the Utermöhl method (Utermöhl, 1958) described by Hasle (1978). The entire chamber surface was scanned at a magnification of x100 to enumerate dinoflagellate species. For dinoflagellates, the limits of detection were 40 and 100 cells $L^{-1}$ for the 25- and 10-mL chambers, respectively. For diatoms, a transect of the chamber was scanned at a magnification of x400 so that the detection limit was 4,545 and 3,636 cells $L^{-1}$ for the Nikon Diaphot and Olympus IX71 microscopes, respectively. For diatoms, the taxonomic nomenclature complied with the register of Algae-base (Guiry and Guiry, 2024; https://www.algaebase.org. Note that only two technicians were in charge of the measurements over the period of interest (from May 2000 to August 2009) and that they performed

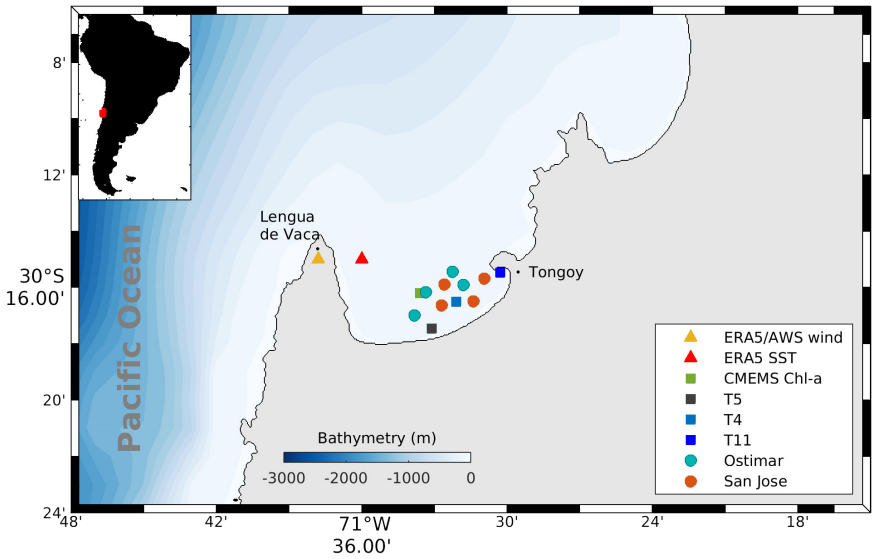


FIGURE 2
Tongoy Bay coastal area and geographic locations of all data utilized in this study, superimposed on the bathymetry field. Circles indicate the eight geographic locations for CTD profile data (temperature and dissolved oxygen) taken from January 2001 to August 2008, recorded by two aquaculture companies (Ostimar and San Jose). Squares indicate the three geographic locations (stations T4, T5, T11) for phytoplankton samples collected between May 2000 and August 2009. Chlorophyll-a data (green square) for the period 2002-2009 was derived from Copernicus Marine Environment Monitoring Service (CMEMS) with 4 km spatial resolution. Yellow triangle placed close to Punta Lengua de Vaca (PLV) indicates the location of the CEAZA weather station and the location of the pixel where wind data was taken from ERA5 reanalysis product. Red triangle indicates the location of the pixel where sea surface temperature (SST) data from ERA5 were taken.

inner calibrations to assess the differences in protocols for counts and taxonomic identification. This gives confidence that analytical biases were minimized. The phytoplankton taxonomy data was partially stored in the SERNAPESCA databases through the Bivalve Mollusk Health Program and by the company OSTIMAR S.A. The Utermöhl method using light microscopy is not ideal for classification of cells according to presence of chloroplasts, as with fluorescence microscopy, and our counts include not only phototrophic and mixotrophic dinoflagellates, but some heterotrophic forms.

Finally, to analyze the changes in community structure, two diversity indices (Simpson and Shannon Weaver) and one evenness index (Pielou) were computed as follows:

Simpson Index formula ($D'si$) (Simpson, 1949):

$$D'si = -\sum_{i=1}^{S} \frac{ni\ (ni-1)}{n\ (n-1)}$$

Where:

$D'si$ = Simpson Index

$ni$ = number of individuals of each species $i$

$n$ = total number of individuals for all $S$ species in the community

Shannon-Weaver Index formula ($H'$) (Shannon and Weaver, 1949):

$$pi = niN$$

$$H' = -\sum_{i=1}^{S}(pi \times log_2 pi)$$

Where:

$H'$= Shannon-Weaver Index

$pi$= the relative importance of species $i$, derived from cell numbers ($n_i/N$)

$ni$= number of individuals of each species $i$

N = total number of individuals for all $S$ species in the community

When H' = 0, the sample contains only one species, and H' will be maximum when all species S are represented by the same number of individuals, that is, that community is a perfectly equitable distribution of abundances (H'max).

Pielou Index formula (Pielou, 1969) is as follows:

$$J' = \frac{H'}{log_2 S}$$

$$H'max = -S(\frac{1}{S} x log_2 \frac{1}{S}) = log_2 S$$

Where:

$H'$ = Shannon-Weaver index

$Log_2 S$ = the maximum diversity ($H'max$) that would be obtained if the distribution of species abundance in the community was perfectly equitable.

When J' = 0, there is no evenness and when J' = 1 there is complete evenness or equitably.

Time series of diatom and dinoflagellate abundances were constructed averaging the cell concentrations enumerated each month. Finally, abrupt changes or increasing trends in diatom and dinoflagellate diversity and evenness over the study period were tested using the non-parametric Pettitt test (Pettitt, 1979) for change-point detection.

## 2.3 Hydrographic data

Hydrographic profiles of temperature and dissolved oxygen (DO) were conducted using a CTD model Ocean Seven 304 Plus Idronaut at eight stations located within Tongoy Bay (Figure 2). Profiles were taken using a Niskin bottle to collect seawater from five discrete depths within the water column: 0, 2, 5, 10, 15 m. Given that the Ostimar S.A and San Jose S.A stations showed a similar variability, either temporally and with depth (not shown), two time series were computed averaging the four stations belonging to Ostimar and the four stations belonging to San Jose (see section 2.1). The time series for both temperature and DO were then correlated to assess the degree of covariation. Pearson correlations for each depth (0, 2, 5 and 10 m) showed higher values for temperature (0.94, 0.94, 0.93 and 0.85, respectively) than DO (0.57, 0.58, 0.53 and 0.5, respectively). Given the high correlations computed between the two time series (i.e. Ostimar and San Jose companies), we estimated one single time series of temperature and DO as representative of seasonal and interannual variability within Tongoy Bay. From these time series, anomalies of temperature and DO (DO*a*) were computed as the difference between any observed value and the long-term (2001–2008) monthly mean value for the same month and depth. Finally, because of notable differences in dissolved oxygen post-2005, and considering the significant oxygen production through phytoplankton photosynthesis, we used a non-parametric Pettitt test (Pettitt, 1979) to evaluate whether (and when) a significant oxygen concentration change occurred during the study period in order to assess potential time synchronicity with changes in phytoplankton biodiversity.

## 2.4 Wind data

Coastal and regional wind variability was characterized by using ERA5 reanalysis product (Hersbach et al., 2020) from the European Center for Medium-Range Weather Forecasts (ECMWF), downloaded from https://rda.ucar.edu/datasets/ds633.0/, for the 10-year study period. The reanalysis of hourly coastal winds was validated against *in-situ* wind records from the CEAZA automatic weather station at the PLV (30.24S, 71.63W), which contains gaps, mainly between 2003 and 2005. To derive the alongshore wind magnitude, the wind components were rotated into a coordinate system that was approximately aligned with the direction of the coast. Subsequently, alongshore wind stress ($\tau_y$) was computed using the following bulk formula:

$$\tau_y = \rho_a \times C_d \times |v| \times \ v$$

where $\rho_a$ is the air density (assumed constant at 1.22 kg m$^{-3}$) and $C_d$ is the neutral drag coefficient varying with the wind magnitude $v$ (Large and Pond, 1981; Gill, 1982). Pearson correlation was used to fit a linear model between daily ERA5 reanalysis and the automatic weather station measurements of alongshore wind and wind-stress, obtaining a good correspondence ($r^2$ = 0.79, see Supplementary Figure S1). Matching the variability in the time and magnitude of the alongshore winds suggests that the ERA5 data correspond well with the *in-situ* wind observations.

Alongshore wind stress was used to calculate the across-shelf Ekman transport ($m$, units = m$^2$ s$^{-1}$ per meter of coast) as follows:

$$m = \frac{1}{\rho_w f} \tau_y \times \ k$$

where $\rho_w$ is the water density (assumed to be constant at 1024 kg m$^{-3}$), $f$ is the Coriolis parameter (s$^{-1}$), and $\tau_y$ and $k$ are the alongshore wind stress and unit vertical vector, respectively. Positive values of $m$ indicate onshore transport due to downwelling favorable winds, whereas negative values indicate offshore transport caused by upwelling favorable winds (Smith, 1968; Bakun, 1973). Additionally, we estimated the Ekman pumping velocity (w, units = m s$^{-1}$) from Smith, 1968:

$$w = \frac{1}{\rho_w f} \nabla \times \tau_y$$

Where $\nabla \times \tau_y$ is the curl of the alongshore wind stress vector. Curl was calculated according to Picket and Paduan (2003). Subsequently, to compare the distribution of both upwelling processes, we converted the Ekman pumping velocities to vertical transport by integrating the vertical velocity along a transect across Tongoy Bay.

## 2.5 Chlorophyll-a and SST data

Surface chlorophyll-a (Chl-a) concentrations were estimated from satellite data provided by the Copernicus Marine Environment Monitoring Service (CMEMS) daily Chl-a product with a spatial resolution of 4 km (European Union-Copernicus Marine Service, 2022). The ERA5 output of sea surface temperature (SST) (Luo and Minnet, 2020) was used to represent the SST variability at the study location. The accuracy of the ERA SST in the study region was validated against the satellite Multi-Scale Ultra High Resolution SST product (Chin et al., 2017) and *in situ* measurements performed with a CTD probe (see section 2.3), giving very good correspondence in both cases (not shown).

## 2.6 Wavelet power spectrum, altimetry data and sea level pressure

We also provide the climatological normalized Wavelet (Morlet) Power Spectrum (WPS) of the intra-seasonal along-shore wind stress anomalies at Tongoy Bay from the ERA5 to assess the peak energy in the synoptic frequency band during the study period. Additionally, sea level anomalies along the equator from altimetry data (2001-2009) were analyzed to indicate the activity of equatorial Kelvin waves propagating from west to east. Finally, annual mean sea level pressure (from the ERA5 reanalysis) was calculated to describe the latitudinal and longitudinal displacement of the SPSA for a broader study period (1940-2023).

## 2.7 Upwelling and downwelling phenology

Two different methodologies were applied to quantify upwelling and downwelling events. For the first approach, upwelling events

were defined as any period with alongshore wind magnitude exceeding a threshold (65$^{th}$ percentile) in the upwelling-favorable direction (i.e., equatorward), while downwelling events implied the same threshold in wind magnitude but in the downwelling-favorable direction (i.e., poleward). The corresponding 65$^{th}$ percentiles of positive (northward) and negative (southward) alongshore wind magnitude were 5 and 2 m s$^{-1}$, respectively. Additionally, any day not included in the upwelling or downwelling range was labeled as a relaxation day (García-Reyes et al., 2014; Cury and Roy, 1989). The number of events and their duration $D_e$ (days) were recorded for each period and season, while the intensity of events was defined as the cumulative wind stress during the event (N m$^{-2}$). The second approach (Tapia et al., 2009) quantifies the synoptic periods of anomalous cold or warm SST that occur during episodes of upwelling or downwelling winds, respectively. Here, synoptic timescales refer to those associated with weather disturbances modulating the along-shore winds off Central Chile. These are tightly linked to the extra-tropical storm activity that induces fluctuations in the winds in the frequency ranges between 2 and 20 days. This represents the main source of intra-seasonal variability in the along-shore wind stress off central Chile (Renault et al., 2012) and at Tongoy Bay (see Supplementary Figure S7). Using the latter methodology, it was possible to estimate the number, duration $D_e$ (days) and intensity (integrated anomaly, °C days) of cooling or warming events in each study period and season (for further details, see Ramajo et al., 2020). Both approaches were used to describe upwelling and downwelling phenology, as they are complementary.

## 2.8 Long-term intra-seasonal variability

Daily time series, long-term monthly means and histograms of low-pass filtered (3-month running average) magnitude, standard deviation, and skewness of the intra-seasonal anomaly were computed to evaluate the relationship between statistical moments, and, to identify any accumulation effect (rectification) of the intra-seasonal variability onto longer timescales of variability. Intra-seasonal anomalies were calculated as the daily departure from the monthly mean, following Dewitte et al. (2011). This implies that intra-seasonal timescales refer to frequencies between 1 and ~ 60 days, and thus include the synoptic timescales. To investigate the relationship between regional and local wind variability, we used standard empirical orthogonal function analysis (Von Storch and Zwiers, 1999) to obtain the statistically dominant mode of the intra-seasonal variability of regional circulation.

# 3 Results

## 3.1 Changes in marine microphytoplankton abundance and diversity over 2000-2009

### 3.1.1 Taxonomic composition of the community of diatoms and dinoflagellates

A total of 126 diatom and 56 dinoflagellate species were identified at T11, T4 and T5. At the genus level, *Chaetoceros* had the highest number of species (27), followed by *Pseudo-nitzschia* (8), *Thalassiosira* and *Rhizosolenia* (7), *Guinardia*, *Coscinodiscus*, *Thalassionema* (4), *Leptocylindrus*, *Bacteriastrum*, *Nitzschia* and *Lauderia* (3). Overall, diatom assemblages were mostly dominated in terms of abundance by *Chaetoceros* (32.4%), *Leptocylindrus* (22%), *Pseudo-nitzschia* (11%) and *Thalassiosira* (5.5%) at station T11; *Chaetoceros* (24%), *Leptocylindrus* (18%), *Pseudo-nitzschia* (17%) and *Skeletonema* (6.3%) at station T4 and *Chaetoceros* (23%), *Pseudo-nitzschia* (19%), *Leptocylindrus* (18%), and *Skeletonema* (9%) at station T5. At species level, *Leptocylindrus danicus*, *Pseudo-nitzschia cf. australis*, *Pseudo-nitzschia cf pungens*, *Chaetoceros debilis*, *Chaetoceros socialis*, *Chaetoceros tortissimus*, *Pseudo-nitzschia delicatissima complex*, *Skeletonema costatum*, *Bacteriastrum delicatulum*, *Thalassiosira aestivalis* and *Asterionellopsis glacialis* reached the highest abundances (> 1 x 10$^6$ cell L$^{-1}$) and accounted for the 81% (T11), 81% (T4) and 86% (T5) of total abundances (See Figure 3). In contrast, diatom species with abundances lower than 1 x 10$^6$ cells L$^{-1}$ accounted for 18% (T11), 18% (T4) and 14% (T5) of the total diatom abundances. Among the species of dinoflagellates identified, the genus *Protoperidinium* showed the highest number of species (4) followed by *Tripos* (2) and *Gyrodinium* (2). Dinoflagellate assemblages were mostly represented by the two species *Dinophysis acuminata* (19%, 12% and 11%) and *Tripos furca* (17%, 13% and 14%) at the T11, T4 and T5 stations, respectively. *Protoperidinium pellucidum* contributed 13% only at T4, *Preperidinium meunieri* contributed to 11% and 9% at T11 and T5, respectively and *Prorocentrum gracile* contributed 11% at station T11. Other unidentified species of dinoflagellates contributed 28%, 35% and 14% to the total abundances at T11, T4 and T5, respectively (See Figure 4). It should be noted that many species of the *Protoperidinium* genus lack chloroplasts, feed heterotrophically, and therefore do not contribute to total chl-a.

### 3.1.2 Seasonal variability and shifts in abundance of diatoms and dinoflagellates

As evidenced from Figures 3 and 4, abundance showed a significant variability that can result from a variety of oceanographic drivers and biological processes. While interannual variability is present, we did not find any significant correlation between the measured variables at Tongoy and typical ENSO indices (Takahashi et al., 2011) over the period 2001-2008 (not shown). This is consistent with the observation that interannual variability in the eastern tropical region (e.g. ENSO) was relatively weak over the period of interest (Lee and MacPhaden, 2010). On the other hand, a long-term trend can be observed in the time series that partly results in a shift in mean conditions around 2005, as will be shown later. Hereafter we will thus focus on seasonal timescales and changes in properties from before and after 2005.

Seasonal variability of diatom and dinoflagellate abundance was evaluated using a non-parametric Mann Whitney test (*U*). Both diatoms and dinoflagellates showed a significant seasonal pattern (See *U* Mann-Whitney in Table 1) where the highest cell concentrations occurred in spring-summer (September to April; mean:1.4 x 10$^6$ cell L$^{-1}$ and October to April; mean: 795 cells L$^{-1}$,

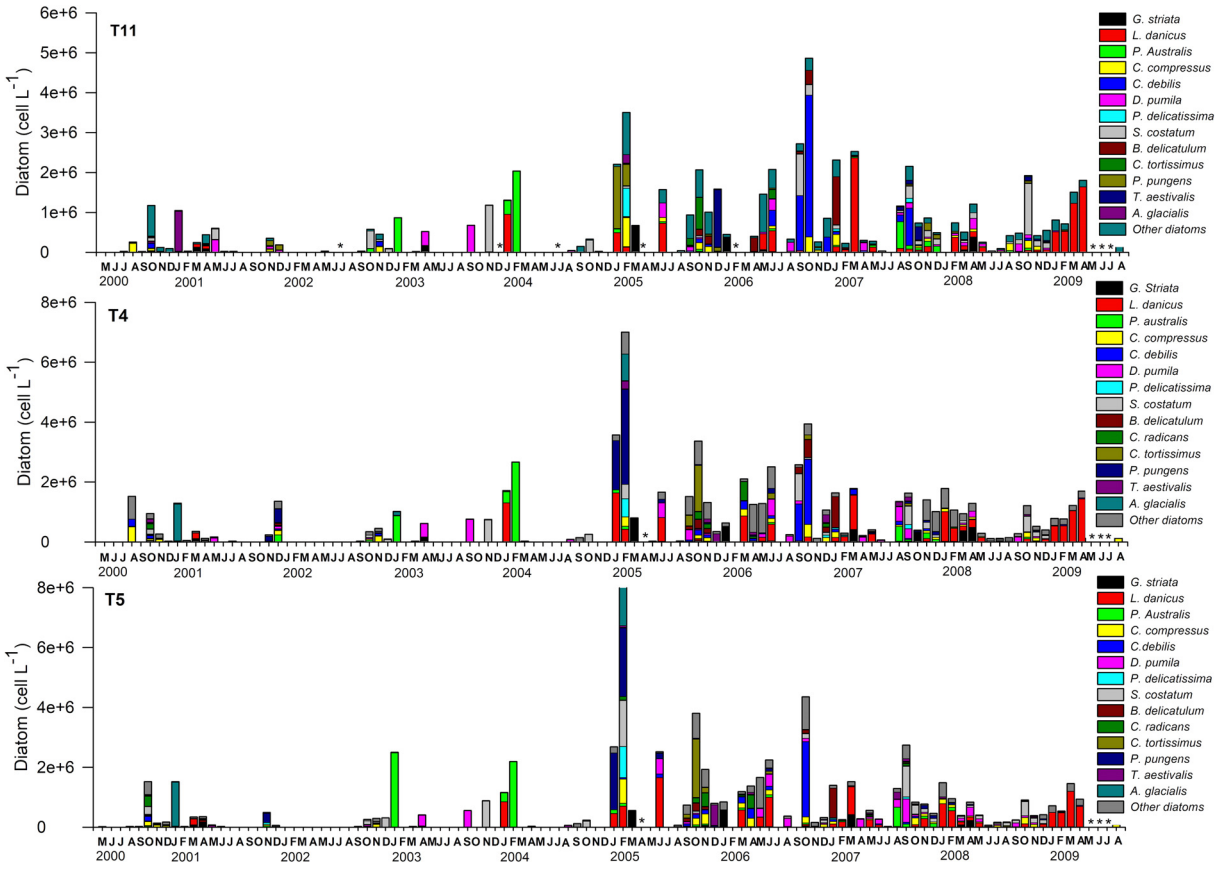


FIGURE 3
Time series of total diatom abundance and taxonomic composition of the main species collected over the first 10 m of the water column from May 2000 to August 2009. Diatoms samples were collected periodically from three stations located in Tongoy Bay; stations T4 (30°16´30" S - 71°32´07" W); T5 (30°17´28" S - 71°33´07" W) and T11 (30°15´28" S - 71°29´50" W). In some months two (fortnightly) or more samplings (weekly) were conducted and in these cases the abundances were averaged. Asterisks indicate missing data, while months without asterisks and no bar indicate that diatom abundances were negligible.

respectively) and the lowest in fall-winter (May to August; mean: 5.6 x $10^4$ cell $L^{-1}$ and May to September; mean: 73 cell $L^{-1}$, respectively) (Table 1). Over a long timescale, both taxa showed a positive trend which was expressed in higher abundances and more frequent productive pulses since January 2005 (diatoms) and in February 2005 or March 2006 (dinoflagellates), depending on the sampling station. The non-parametric Mann-Whitney test (U) showed that both diatoms and dinoflagellates showed significant interannual differences ($p < 0.05$; See Table 1), suggesting an oceanographic regime change post-2005.

### 3.1.3 Seasonal variability and shifts in community composition of diatoms and dinoflagellates

Seasonal variability of the relative contribution of diatom species showed that summer was mainly dominated by *Leptocylindrus danicus* (32%), *Pseudo-nitzschia australis* (16%), *Pseudo-nitzschia pungens* (10%) and *Guinardia striata* (6%), autumn dominated by *Leptocylindrus danicus* (34%), *Detonula pumila* (8%) and *Guinardia striata* (7%), winter dominated by *Chaetoceros debilis* (25%), *Skeletonema costatum* (16%), *Detonula Pumila* (15%) and *Pseudo-nitzschia australis (8%)* and spring dominated by *Chaetoceros debilis* (22%), *Skeletonema costatum* (21%), *Thalassiosira aestivalis* (10%) and *Chaetoceros compressus* (7%). For dinoflagellate taxa, autumn was mainly dominated by *Scrippsiella trochoidea* (55%) and *Heterocapsa* sp. (11%); winter dominated by *Heterocapsa* sp. (25%), *Prorocentrum gracile* (18%), *Protoperidinium* sp. (17%) and *Protoperidinium divergens* (11%); spring dominated by *Gymnodinium* sp. (20%), *Protoperidinium* sp. (30%) and *Protoperidinium depressum* (15%), and summer dominated by *Prorocentrum gracile* (37%), *Prorocentrum micans* (18%) and *Heterocapsa* sp. (16%).

Beside seasonal variations, the abundance of diatoms (>1 x $10^6$ cells $L^{-1}$) evidenced a marked increase from January 2005 (Figure 3). In order to quantify such a change, we consider average quantities over the periods prior to and after 2005, i.e. period 1 (that is, May 2000 to December 2004) and period 2 (January 2005 to August 2009). During period 1, there is an important relative contribution of the harmful species *Pseudo-nitzschia australis* in Tongoy Bay accounting for 27% (T11), 28% (T4) and 37% (T5), respectively followed by *Skeletonema costatum* with a contribution of 19% (T11), 10% (T4), 13% (T5) and *Detonula Pumila* with 12% (T11), 10% (T4), 10% (T5), respectively. Period 2 (i.e. January 2005 to August 2009) was dominated by *Leptocylindrus danicus* at 20% (T11), 26% (T4) and 20% (T5), followed by *Chaetoceros debilis* at 4% (T11), 8% (T4) and

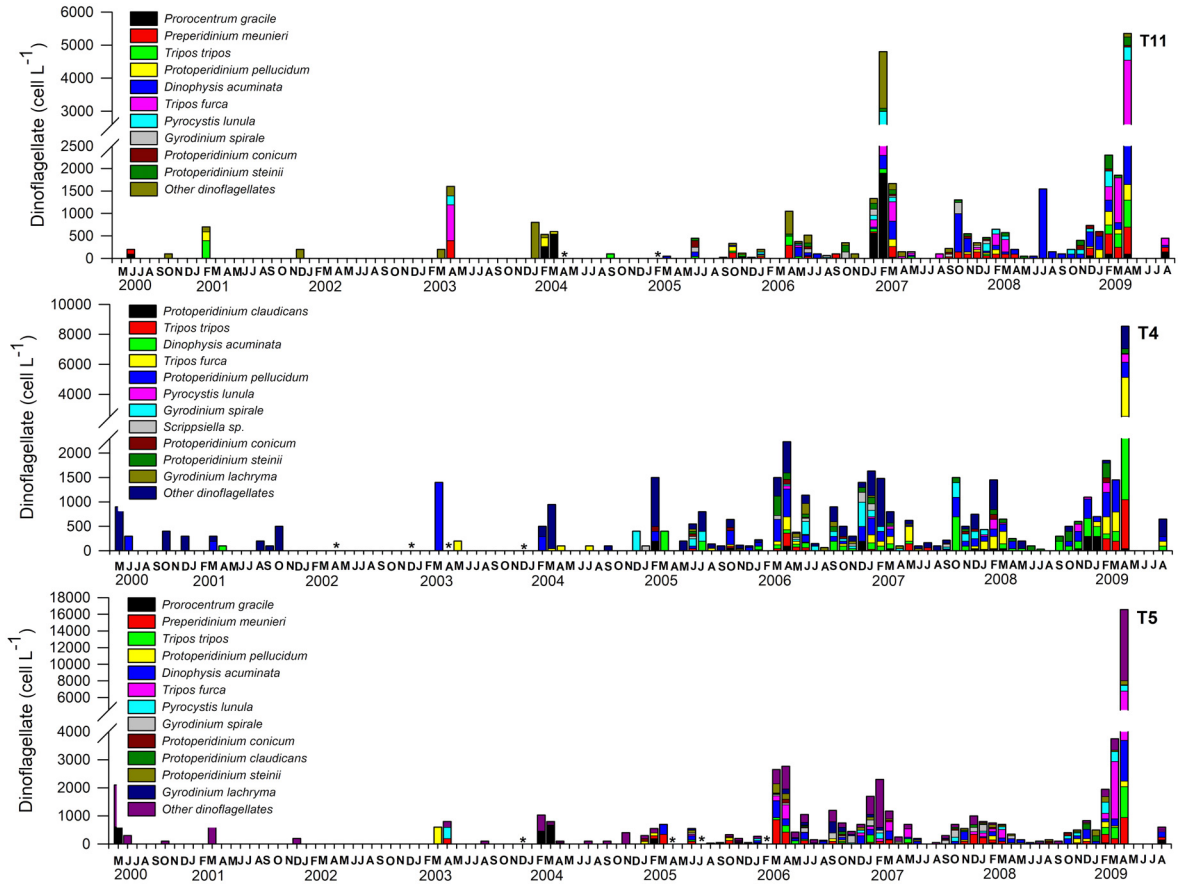


FIGURE 4
Time series of total dinoflagellate abundance and taxonomic composition at Tongoy Bay over the first 10 m of the water column from May 2000 to August 2009. Dinoflagellate samples were collected periodically from three stations located in Tongoy Bay; stations T4 (30°16´30" S - 71°32´07" W); T5 (30°17´28" S - 71°33´07" W) and T11 (30°15´28" S - 71°29´50" W). In some months two (fortnightly) or more samplings (weekly) were conducted and in these cases the abundances were averaged. Asterisks indicate missing data, while months without asterisks and no bar indicate that diatom abundances were negligible.

7% (T5), *Skeletonema costatum* at 8% (T11), 6% (T4), and 8% (T5) and *Pseudo-nitzschia pungens* at 6% (T11), 10% (T4) and 9% (T5). Between periods 1 and 2, some species such as *Leptocylindrus danicus* increased their relative contribution from 9% to 20%, whereas other diatom species, such as, *Pseudo-nitzschia australis* decreased in relative contribution from 37% to 3% in T5, 27% to 3% in T11 and 28% to 2% in T4. Diatoms of the genus *Pseudo-nitzschia* have been recognized globally as responsible for amnesic shellfish poisoning (ASP), and more specifically *P. australis* has been recognized as the most important producer of ASP in the coastal upwelling ecosystem of northern Chile (Alvarez et al., 2020). Our findings showed that *Pseudo-nitzschia* spp. (i.e. *P. australis, P. pungens, P. delicatissima complex*) were present throughout the entire monitoring period but reached the highest densities during period 1 and during the transition-time between period 1 and period 2. In some cases, blooms were dominated exclusively by *P. australis*: January 2003 (2.48 x $10^6$ cells $L^{-1}$) and February 2004 (2.19 x $10^6$ cells $L^{-1}$) and others partially by *P. pungens*: January 2005 (1.9 x $10^6$ cells $L^{-1}$) and February 2005 (2.3 x $10^6$ cell $L^{-1}$). *Pseudo-nitzschia* spp. cells occurred in mixed blooms from May-2005 onwards (period 2) with abundances less than 7 x $10^5$ cells $L^{-1}$. The relative contribution of dinoflagellate species showed that period 1 was dominated by *Scrippsiella trochoidea* (15%), *Prorocentrum gracile* (13%), *Prorocentrum micans* (12%), *Protoperidinium pellucidum* (14%) and *Ceratium furca Var. Berghi* (11%) whereas period 2 was mainly dominated by *Dinophysis acuminata* (18%), *Ceratium furca Var. Berghi* (14%), *Diplopsalis lenticula* (9%) and *Prorocentrum gracile* (8%) (See Figure 4).

### 3.1.4 Diversity and evenness indices of the community of diatoms and dinoflagellates

Diversity and evenness indices of the community of diatoms and dinoflagellates were significantly higher during period 2 than period 1 in both diatom and dinoflagellate groups at the three stations (T11, T4, T5); however, the variability (coefficient of variation; CV%) was higher in period 1 than in period 2 (See Table 2). The application of the Pettitt test to detect significant change points within the time series of Simpson and Shannon-Weaver indices (only computed for diatoms) showed similar results for both indices at all three stations (T11, T4 and T5) (see Supplementary Figure S2). Here, both diversity indices showed a significant increase ($p < 0.05$) between May and June 2005 at

10.3389/fmars.2024.1434007

TABLE 1 A non-parametric Mann-Whitney test (U) was used to assess seasonal differences in microphytoplankton abundances.

| Functional group | Period | Statistics/U Mann-Whitney test | Period 1 2000 - 2004 | Period 2 2005 - 2009 |
|---|---|---|---|---|
| *Diatom* | *Low productive (LP) Season* (MayA-August)<br><br>*High productivity (HP) Season* (September-April) | Mean (cell $L^{-1}$)<br>Range (cell $L^{-1}$)<br>CV (%)<br>Mean (cell $L^{-1}$)<br>Range (cell $L^{-1}$)<br>CV (%)<br>Seasonal *U* (LP *vs* HP)<br>*P*<br>$n_1$, $n_2$ | $5.6 \times 10^4$<br>11 – 1519586<br>385%<br>$3.7 \times 10^5$<br>21 – 2667927<br>154%<br>1737<br>**0.000008**<br>57, 106 | $5.4 \times 10^5$<br>7910 – 2519747<br>134%<br>$1.4 \times 10^6$<br>119482 – 9523866<br>100%<br>1033<br>**0.000**<br>50, 99 |
| | | Interannual *U* (P1 *vs* P2)<br>*P*<br>$n_1$, $n_2$ | 4101<br>**0.000**<br>163, 149 | |
| *Dinoflagellate* | *Low-productivity (LP) Season* (MayS-September)<br><br>*High productivity (HP) Season* (October – April) | Mean<br>Range<br>CV (%)<br>Mean (cell $L^{-1}$)<br>Range (cell $L^{-1}$)<br>CV (%)<br>Seasonal *U* (LP *vs* HP)<br>*P*<br>$n_1$, $n_2$ | 73<br>0 – 2100<br>404%<br>157<br>0 – 1600<br>209%<br>2696<br>**0.021**<br>60, 108 | 589<br>0 - 16550<br>364%<br>795<br>0 – 8550<br>150%<br>2096<br>**0.000341**<br>60, 105 |
| | | Interannual *U* (P1 *vs* P2)<br>*P*<br>$n_1$, $n_2$ | 5337<br>**0.000**<br>168, 144 | |

Shifts in diatom and dinoflagellate abundances were also assessed between two periods: May 2000- December 2004 (Period 1) and January 2005- August 2009 (Period 2). Bold text *P* and *n* show significant P-values at $\alpha = 0.05$ and number of samples, respectively.

TABLE 2 Diversity (i.e. Simpson and Shannon-Weaver) and evenness (i.e. Pielou) indices computed for times series of microphytoplankton abundance from stations ($S_t$) T11, T4 and T5 at Tongoy Bay (See Figure 2).

| Functional group | $S_t$ | Diversity and evenness indices | Period 1 2000 - 2004 | | | | | Period 2 2005 - 2009 | | | | |
|---|---|---|---|---|---|---|---|---|---|---|---|---|
| | | | Mean | Min | Max | S.D | CV (%) | Mean | Min | Max | S.D | CV (%) |
| *Diatom* | T11 | *Simpson* | 0.47 | 0.005 | 0.92 | 0.26 | 54 | 0.59 | 0 | 0.87 | 0.25 | 42 |
| | | *Shannon-Weaver* | 1.39 | 0.025 | 4.23 | 0.93 | 67 | 1.92 | 0 | 3.47 | 0.96 | 50 |
| | | *Pielou* | 0.62 | 0.025 | 0.93 | 0.29 | 46 | 0.67 | 0.17 | 1 | 0.22 | 33 |
| | T4 | *Simpson* | 0.47 | 0 | 0.88 | 0.26 | 55 | 0.6 | 0 | 0.9 | 0.22 | 37 |
| | | *Shannon-Weaver* | 1.35 | 0 | 3.42 | 0.84 | 62 | 1.98 | 0 | 3.79 | 0.86 | 44 |
| | | *Pielou* | 0.62 | 0.003 | 0.98 | 0.28 | 45 | 0.66 | 0.43 | 0.94 | 0.17 | 26 |
| | T5 | *Simpson* | 0.44 | 0 | 0.87 | 0.27 | 61 | 0.62 | 0.06 | 0.89 | 0.2 | 33 |
| | | *Shannon-Weaver* | 1.28 | 0 | 3.51 | 0.82 | 64 | 1.98 | 0.2 | 3.63 | 0.78 | 40 |
| | | *Pielou* | 0.59 | 0.01 | 0.98 | 0.3 | 51 | 0.66 | 0.2 | 1 | 0.19 | 29 |
| *Dinoflagellate* | T11 | *Simpson* | 0.29 | 0 | 0.37 | 0.26 | 89 | 0.65 | 0 | 0.87 | 0.26 | 40 |
| | | *Shannon-Weaver* | 0.67 | 0 | 0.81 | 0.65 | 95 | 2.0 | 0 | 3.33 | 1.01 | 50 |
| | | *Pielou* | 0.11 | 0 | 0.14 | 0.11 | 100 | 0.34 | 0 | 0.57 | 0.17 | 50 |
| | T4 | *Simpson* | 0.11 | 0 | 0.56 | 0.23 | 205 | 0.62 | 0 | 0.88 | 0.29 | 46 |
| | | *Shannon-Weaver* | 0.28 | 0 | 1.37 | 0.6 | 212 | 1.94 | 0 | 3.45 | 1.08 | 56 |

*(Continued)*

TABLE 2 Continued

| Functional group | $S_t$ | Diversity and evenness indices | Period 1 2000 - 2004 | | | | | Period 2 2005 - 2009 | | | | |
|---|---|---|---|---|---|---|---|---|---|---|---|---|
| | | | Mean | Min | Max | S.D | CV (%) | Mean | Min | Max | S.D | CV (%) |
| | | *Pielou* | 0.04 | 0 | 0.23 | 0.1 | 255 | 0.33 | 0 | 0.59 | 0.18 | 56 |
| | T5 | *Simpson* | 0.14 | 0 | 0.65 | 0.28 | 200 | 0.66 | 0 | 0.89 | 0.23 | 35 |
| | | *Shannon-Weaver* | 0.34 | 0 | 0.99 | 0.68 | 200 | 1.99 | 0 | 3.48 | 0.91 | 45 |
| | | *Pielou* | 0.05 | 0 | 0.25 | 0.12 | 200 | 0.34 | 0 | 0.6 | 0.16 | 46 |

For each sampled station, two functional groups were analyzed: diatoms and dinoflagellates. The statistical mean, standard deviation (SD), coefficient of variation (CV) and minimum and maximum values were computed for period 1 (2000- 2004) and period 2 (2005- 2009).

stations T4 and T5 (see Supplementary Table S1). As for the Pielou index, two shifts in the mean were identified: April 2002/May 2005, April 2002/May 2007 and June 2002/May 2005 at stations T4, T11 and T5, respectively; however, the changes observed in April 2002 (T4 and T11), June 2002 (T5) and May 2007 at station T11 show a non-significant change (Supplementary Table S1).

#### 3.1.5 Annual cycles of abundances of diatoms and dinoflagellates

We compared the monthly averages of the diatom and dinoflagellate abundances between period 1 and period 2 to identify changes in the phenology of the productive pulse. Diatom abundance was generally one order of magnitude higher in period 2 (~1 x $10^6$ cells $L^{-1}$) than in period 1 (~1 x $10^5$ cells $L^{-1}$) (with the exception of January where average abundance in period 1 was also ~1 x $10^6$ cells $L^{-1}$) (Figure 5). Several peaks in diatom abundances (>1 x $10^6$ cells $L^{-1}$) occurred during period 2, which notably contrasted with period 1, where diatom abundances were relatively low around the year, with the exception of the peak in January (Figure 5). The monthly means in dinoflagellate abundance showed several peaks, especially in February and April during period 2, with cell abundances > 1500 cells $L^{-1}$. During period 1, dinoflagellate abundances showed lower peaks (<1000 cells $L^{-1}$) in February/March and May (See Figure 6). Finally, the coefficient of variation (CV) of the mean monthly abundances of diatoms and dinoflagellates both showed higher variability in period 2 than in period 1.

# 4 Environmental drivers

## 4.1 Seasonal and annual timescales

### 4.1.1 Hydrographic conditions

Temperature displayed a seasonal cycle with maxima occurring in September-February (late winter/spring-summer) and minima in March-August (late summer/fall- winter) (see Figure 7A). The dissolved oxygen (DO) time series (see Figure 7C) displayed a marked seasonal pattern with concentrations ranging between 8 – 11.5 mg $L^{-1}$ during spring-summer seasons. A Pettitt test applied to this time series indicated that post-May 2005, DO increased significantly ($K_T$= 959; p= 0.001805) in the upper 15 m of the water column. After June 2005, second and third DO change points were detected in March 2007 ($K_T$= 184; p= 0.07096) and September 2007 ($K_T$= 66; p= 0.02865), respectively. The statistical averages of DO anomalies (DO*a*) computed for the three periods between change points are detailed as follows: January 2001 to May 2005 (DO*a*= -0.36 mg $L^{-1}$), June 2005 to February 2007 (DO*a*= 0.79 mg $L^{-1}$), March to August 2007 (DO*a*= -0.88 mg $L^{-1}$) and September 2007 to August 2008 (DO*a*= 0.42 mg $L^{-1}$). This indicates that post-2005 the oxygen concentrations exhibited abrupt changes in the upper layer, particularly between March and August 2007, and this may be interpreted as resulting from the La Niña conditions present in 2007-2008 (See Figure 7B). These conditions were associated with enhanced upwelling Kelvin wave activity in the equatorial Pacific (See Supplementary Figure S3), an increase in the poleward transport of oxygen-poor waters by the Peru–Chile undercurrent (Pizarro-Koth et al., 2023), and an increased strength of the SPSA in 2007 (See Supplementary Figure S4) as also reported by Schneider et al. (2017) for a coastal upwelling system off Concepción (36°S).

### 4.1.2 Alongshore wind stress, Ekman transport, Ekman pumping, SST

Hereafter we document the variability of alongshore wind stress and derived quantities, along with SST, focusing principally on observed changes in properties before and after 2005. To describe the variability of the upwelling in Tongoy Bay, daily time series were analyzed for alongshore wind stress ($\tau_y$), Ekman transport (m), Ekman Pumping (w) and Sea Surface Temperature (SST). Daily $\tau_y$ at Punta Lengua de Vaca (PLV) showed year-round southerly episodes (see positive values in Supplementary Figure S5A) that induced upwelling pulses reflected in the offshore Ekman transport (see negative values in Supplementary Figure S5B). However, during the spring and summer months, the frequency and amplitude of upwelling-favorable $\tau_y$ and offshore transport increased. Additionally, in the fall and winter months the southerly winds alternated with periods of northerly downwelling-favorable winds (see negative $\tau_y$ and positive transport in Supplementary Figures S5A, B, respectively). On the other hand, upwelling transport by Ekman pumping (i.e. negative clockwise wind stress curl), integrated over a transect across Tongoy Bay, was also evident throughout the year, but lower in magnitude than offshore Ekman transport and alternating with downwelling activity (i.e. positive counterclockwise wind stress curl) in

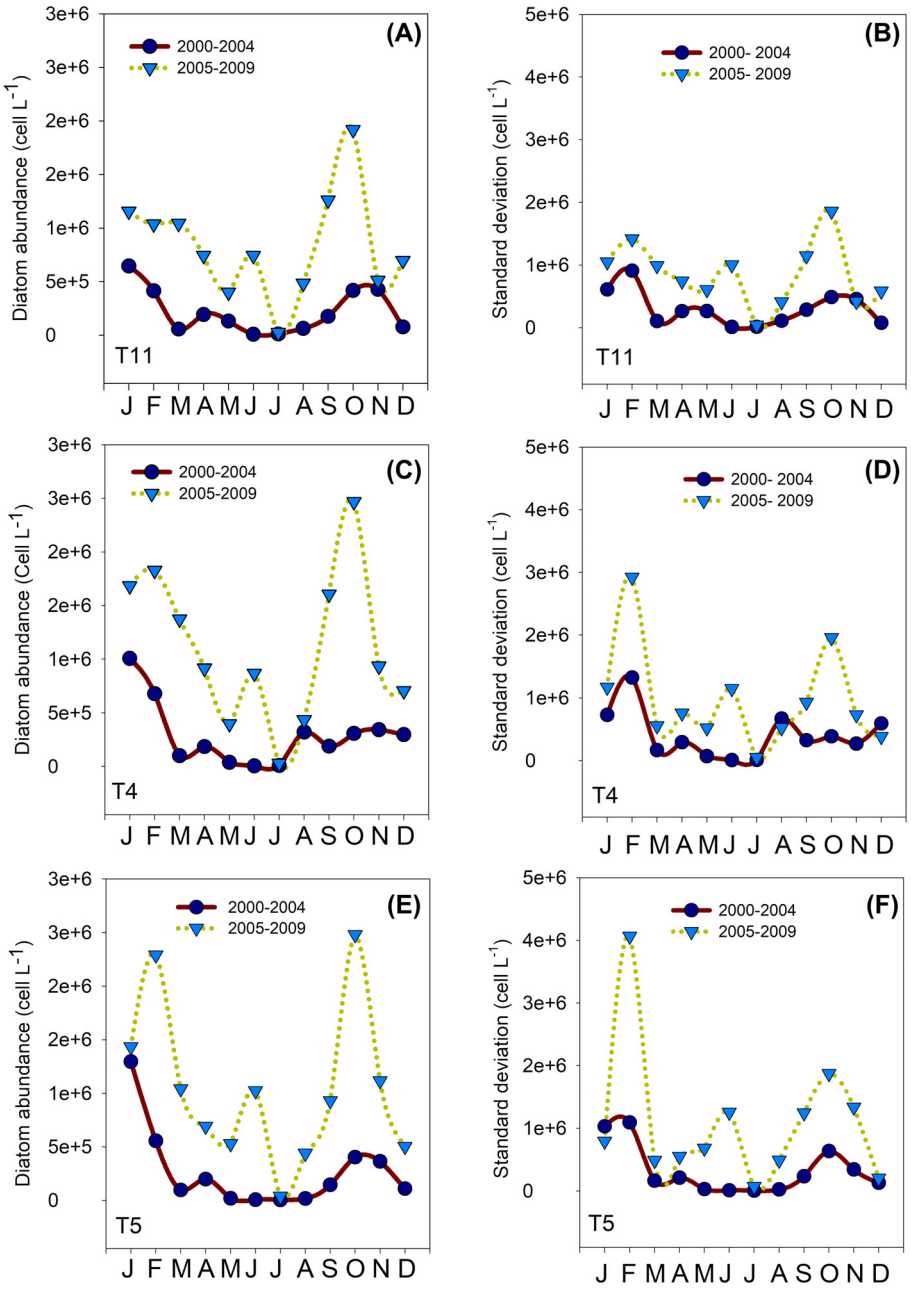


FIGURE 5
Monthly mean **(A, C, E)** and standard deviation **(B, D, F)** of diatom abundances as a function of calendar month at stations T4 (30°16´30" S - 71°32´07" W); T5 (30°17´28" S - 71°33´07" W) and T11 (30°15´28" S - 71°29´50" W) in Tongoy Bay. Averages and standard deviations were computed for two different periods: May 2000- December 2004 (dark blue circles) and January 2005- August 2009 (blue down triangle) showing the abrupt increase of the diatom abundances observed post-2005 (See Figures 2, 3).

wintertime because of the increase in northerly $\tau_y$ (see Supplementary Figure S5C). For SST, the annual cycle showed marked seasonal variability, with maximum in summer and minimum in winter following the annual cycle of solar radiation (Supplementary Figure S5D; Shaffer et al., 1999).

Given the abrupt changes in abundance of diatoms and dinoflagellates observed since 2005, differences between the study periods were analyzed. The long-term monthly mean ($\tau_y$, Ekman transport/pumping and SST) and statistics (i.e., mean, median, standard deviation and skewness) by period are shown in Figure 8 and summarized in Supplementary Table S2, respectively. On average, the monthly means of $\tau_y$ and associated Ekman processes exhibited permanent upwelling-favorable conditions during both periods, however during period 2, the values were higher and less variable than during the first period, particularly, between May and October (see Figure 8). In terms of the relative contributions of Ekman processes to coastal upwelling in the study area, the mean Ekman pumping was ~55% lower than mean Ekman transport in both study periods, however, their summed mean contributions were higher during period 2 (0.487 $m^3$ $s^{-1}$ *vs* 0.503 $m^3$ $s^{-1}$ in 2000-2004 and 2005-

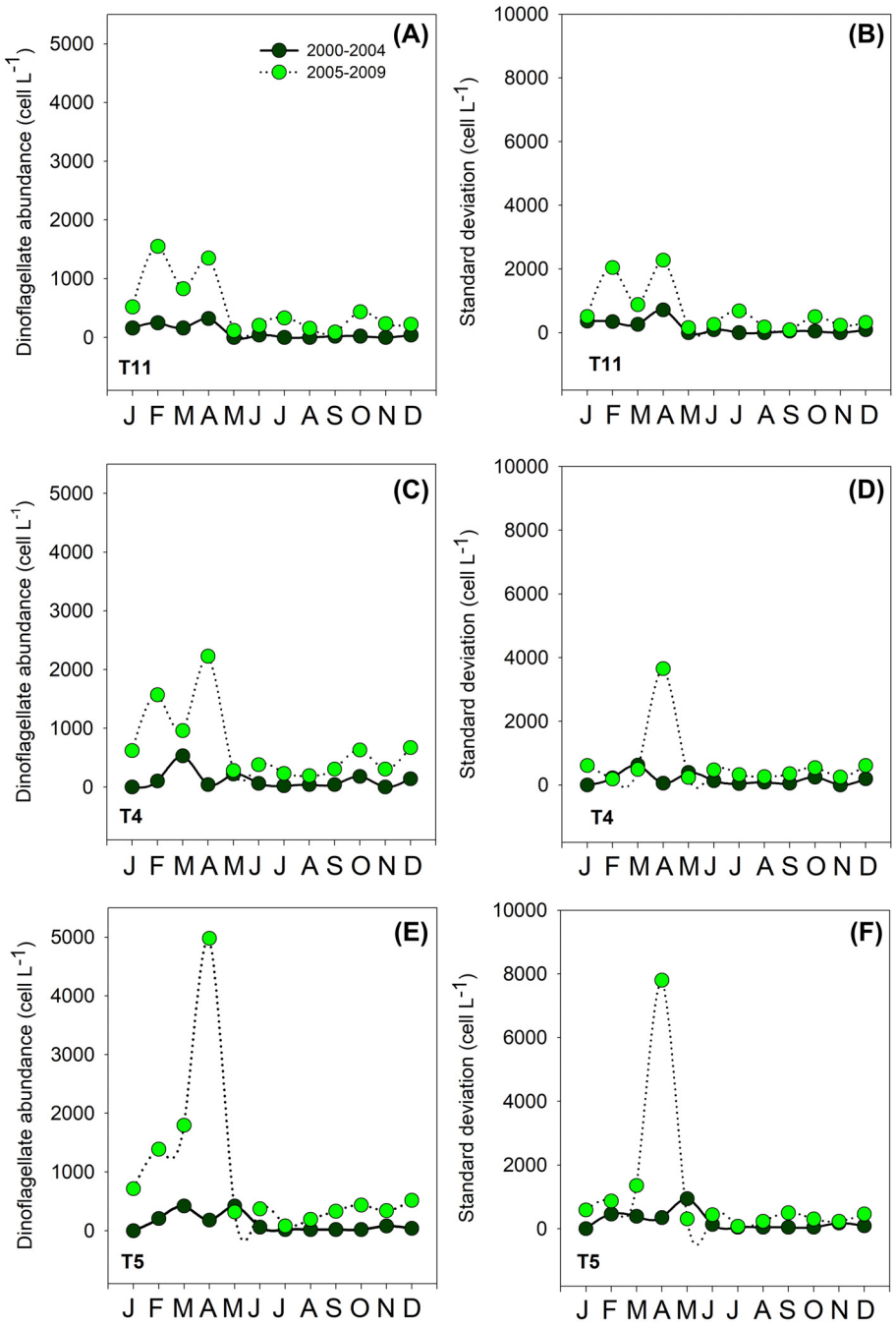


FIGURE 6
Monthly mean **(A, C, E)** and standard deviation **(B, D, F)** of dinoflagellate abundance as a function of calendar month at stations T4 (30°16´30" S - 71° 32´07" W); T5 (30°17´28" S - 71°33´07" W) and T11 (30°15´28" S - 71°29´50" W) in Tongoy Bay. Averages and standard deviations were computed for two different periods: May 2000- December 2004 (dark green circles) and January 2005- August 2009 (light green circles) showing the change in properties (i.e., higher abundances and frequency) post-2005 (See Figures 2, 4).

2009, respectively). Additionally, the frequency distributions (not shown) of daily $\tau_y$ and Ekman transport/pumping, were more skewed toward downwelling-favorable conditions during the earlier period, in partduring the fall-winter seasons (see Supplementary Table S2 and Supplementary Figure S5). The second period, however, was characterized by skewness values corresponding to more upwelling-favorable conditions. On the other hand, SST showed an increase in the mean variability and a broadening distribution from period 1 to period 2 (Supplementary Table S2). The amplitude of the SST annual cycle, based on monthly averages, was larger in period 2, with a ratio between maximum and minimum reaching 4°C and 5°C in the first and second periods, respectively (Figure 8).

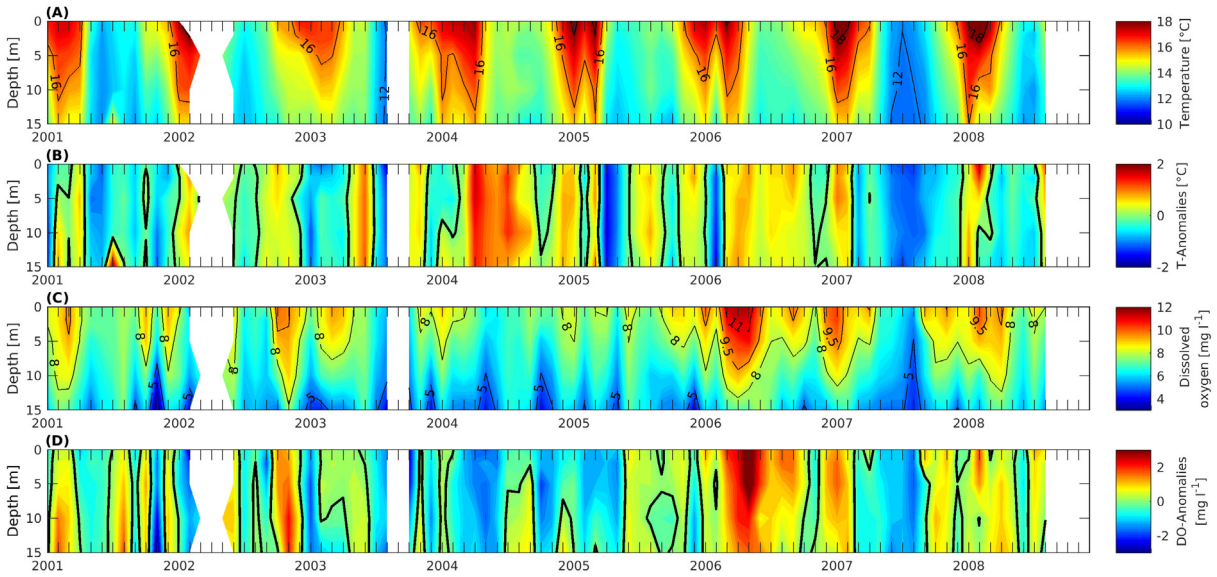


FIGURE 7
Time-series of oceanographic variables recorded in Tongoy Bay from January 2001 to August 2008 for the upper layer (0-15 m depth): **(A)** Temperature. **(B)** Temperature anomalies. **(C)** Dissolved oxygen and **(D)** Dissolved oxygen anomalies. The bold black line on **(B, D)** represents the contour for zero anomaly. See Section 2.3 for the details of the construction of time series.

### 4.1.3 Upwelling/relaxation/ downwelling phenology

The coastal upwelling and downwelling activity in Tongoy Bay were quantified by period (i.e., 2000-2004 and 2005- 2009) and season (fall-winter and spring-summer) using two indices based on: (i) daily $\tau_y$ magnitude and (ii) synoptic SST anomalies (Tapia et al., 2009) (see Tables 3, 4, respectively). On a seasonal scale, the $\tau_y$ index indicated a slightly higher number of upwelling events in fall-winter, although with lower cumulative duration (days) and intensity (N $m^{-2}$) than in spring-summer during both study periods. On the other hand, the results indicate comparable total frequency, duration and intensity values between the first and second study periods; however, the fall-winter (spring-summer) seasons during the years 2005-2009 exhibit more (less) upwelling activity than during the years 2000-2004. More remarkable are the statistical differences in the downwelling and relaxation events, in the first case, downwelling episodes were mostly concentrated in the autumn-winter period, with 81 and 92% of occurrence in those seasons during the first and second periods, respectively; it is worth noting the reduction of southward forcing (downwelling) in the second period by 42%, 48% and 56% in frequency, temporal duration and intensity, respectively (see Table 3). Regarding the relaxation events, a similar frequency was observed between both study periods, with a slight increase in the autumn and winter seasons in relation to the spring-summer; however, in terms of temporal duration and intensity of the relaxation episodes, the second period (2005-2009) showed higher values in all seasons.

### 4.1.4 Sea surface temperature index

The analysis of synoptic cold or warm SST anomalies in concomitance with periods of intensified upwelling (northward wind above the 65th percentile, i.e., 5 m $s^{-1}$) or downwelling favorable wind (southward wind above the 65th percentile, i.e., 2 m $s^{-1}$), respectively, indicates the predominance of warm (cold) anomalies in fall-winter (spring-summer) seasons (Table 4). On the other hand, the study periods differ markedly with a reduction of 43, 46 and 44% in frequency, temporal duration and intensity of the warming episodes, respectively, during period 2 (2005-2009), and an increase in frequency and intensity of cooling events of 30 and 16% respectively. Note that this particular index is not a proxy for coastal upwelling, in contrast to the $\tau_y$ index; instead, this index provides a metric for the relationship between the local thermal variability and biological properties modulated by environmental conditions (Tapia et al., 2009).

### 4.1.5 Annual cycles of the upwelling/relaxation/ downwelling events

To deepen the analysis of upwelling, downwelling and relaxation events, we analyzed in Figure 9 the cumulative frequency and intensity of these episodes, classifying by month and temporal duration (we separated events into three categories: short (≤ 3 days), medium (4–10 days), and long events (>10 days), and by study period (period 1 *vs* period 2). Firstly, in terms of cumulative frequency, upwelling events of short duration dominated both periods with an increase in the number of medium duration episodes in the winter and spring seasons (from June to December). Secondly, cumulative upwelling intensity showed a seasonal pattern during both periods characterized by an increase in intense medium and long-duration upwelling episodes in winter and spring (June to December). Cumulative upwelling intensity reached higher values during period 2 compared with period 1 in August, September and October. On the other hand, relaxation episodes showed a greater frequency of longer events (> 10 days) during the spring and summer in both periods, but were more frequent in period 2 (Figure 9). Generally, an increase in the intensity of longer relaxation episodes predominated during the spring to early autumn seasons (November to May) in both periods, although period 2 showed the

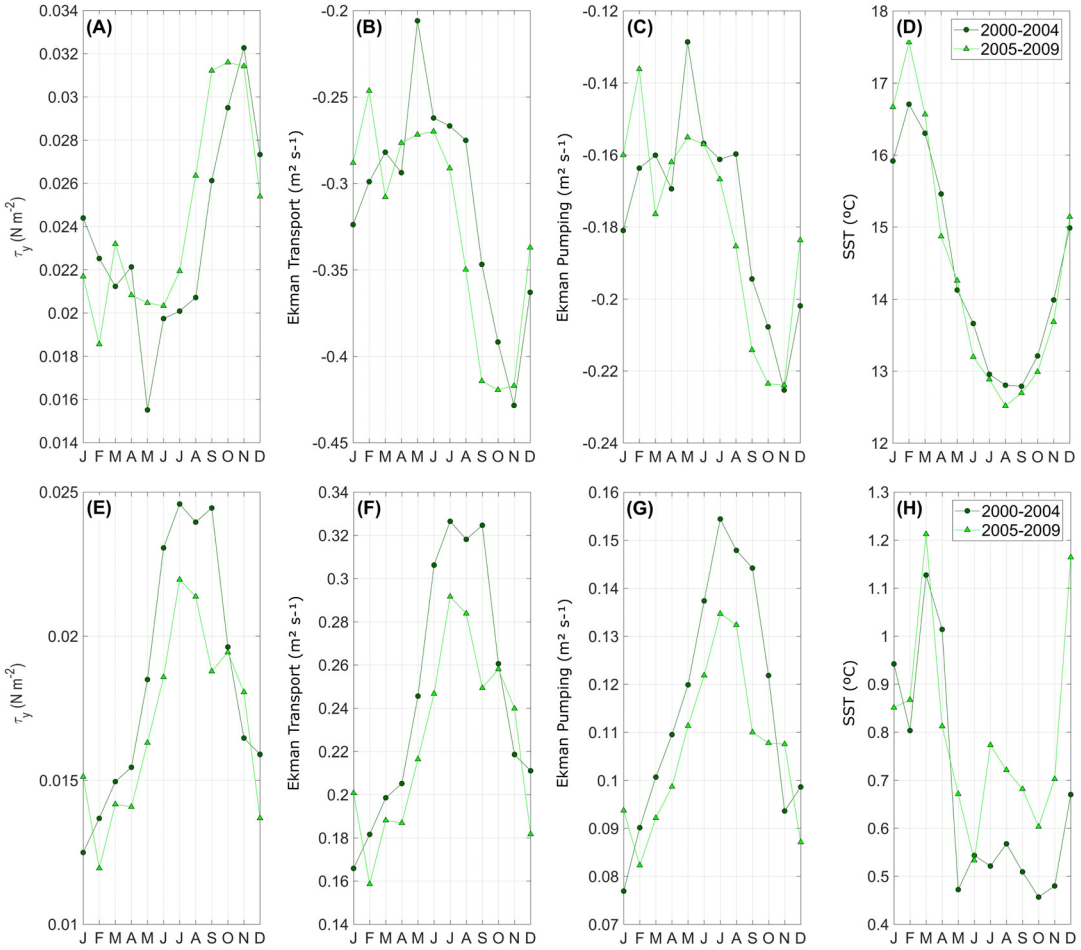


FIGURE 8
Long-term monthly means of magnitude **(A-D)** and standard deviation **(E-H)** as a function of calendar month for: **(A, E)** Alongshore wind stress (N m$^{-2}$) and **(B, F)** Ekman transport (m$^2$ s$^{-1}$ per meter of coast) with negative values as offshore transport (upwelling favorable winds) at Punta Lengua de Vaca (PLV). Data are taken from ERA5. **(C, G)** Vertical transport by Ekman pumping (m$^2$ s$^{-1}$ per meter of coast) at a transect through Tongoy Bay. **(D, H)** Sea Surface Temperature (SST) at Tongoy Bay. Long-term monthly means were computed for two different study periods: from January 2000 to December 2004 (dark green) and from January 2005 to December 2009 (light green). Vertical transport by Ekman pumping **(C)** is shown multiplied by -1 to enable a comparison with Ekman Transport **(B)**.

longest relaxation events. Finally, we highlight the lower frequency and intensity of downwelling events observed during the second period, compared to the first period in the autumn and winter months.

## 4.2 Intra-seasonal winds/SST variability

In addition to the influences of the interannual and seasonal regimes, coastal winds and upwelling responses at Tongoy Bay are principally linked to changes in atmospheric circulation on intra-seasonal and synoptic time scales (Renault et al., 2009; Rahn, 2012). These can be modulated at interannual and decadal timescales, which can alter upwelling conditions. To explore the interannual fluctuations in intra-seasonal variability, the daily alongshore wind stress ($\tau_y$) Intra-Seasonal Anomaly (ISA) was calculated, together with the 3-month running mean, standard deviation and skewness (Supplementary Figure S6). Firstly, the running mean of the absolute value and standard deviation of the $\tau_y$ ISA exhibited a sharp reduction during period 2 (2005-2009), especially during the austral fall-winter seasons (Supplementary Figures S6A, B). In addition, the evolution of the running skewness of the $\tau_y$ ISA also exhibited a notable modification between the two periods (Supplementary Figure S6C). These changes are clearly visible in the monthly mean climatology of these time series (Figure 10). In particular, the mean absolute value and standard deviation of the $\tau_y$ ISA exhibited a sharp reduction and positive skewness along the annual cycle during period 2 (2005-2009). We also verified that the wavelet power of $\tau_y$ ISA decreased significantly from the period 2000-2004 to the period 2005-2009 (see Supplementary Figure S7). These findings suggest notable changes in the intra-seasonal alongshore wind phenology in Tongoy Bay post-2005.

## 4.3 Decadal variability of low and high frequency winds

In this section, the interannual to decadal variability of alongshore wind stress and SST off Central Chile is analyzed to evaluate the extent

10.3389/fmars.2024.1434007

TABLE 3 Indices for upwelling, relaxation and downwelling events based on daily alongshore wind stress in Tongoy Bay.

| Alongshore wind stress ( $\tau_y$) index | | | | | | | | | | |
|---|---|---|---|---|---|---|---|---|---|---|
| Period | | Upwelling events | | | Relaxation events | | | Downwelling events | | |
| | | N° (#) | Cumulative Duration $D_e$ (days) | Cumulative Intensity (N $m^{-2}$) | N° (#) | Cumulative Duration $D_e$ (days) | Cumulative Intensity (N $m^{-2}$) | N° (#) | Cumulative Duration (days) | Cumulative Intensity (N $m^{-2}$) |
| 2000 - 2004 | Fall -winter | 123 | 278 | 11.93 | 157 | 586 | 7.73 | 35 | 56 | -1.36 |
| | Spring -summer | 118 | 342 | 15.37 | 138 | 554 | 9.43 | 8 | 11 | -0.26 |
| | Total | 241 | 620 | 27.3 | 295 | 1140 | 17.16 | 43 | 67 | -1.62 |
| 2005 - 2009 | Fall - winter | 125 | 295 | 12.53 | 159 | 594 | 8.5 | 22 | 31 | -0.61 |
| | Spring - summer | 114 | 325 | 14.63 | 133 | 577 | 9.67 | 3 | 4 | -0.1 |
| | Total | 239 | 620 | 27.16 | 292 | 1171 | 18.17 | 25 | 35 | -0.71 |

Within each study period (1 and 2) and season, upwelling (downwelling) events were identified as episodes when the daily southerly (northerly) alongshore wind exceeded and remained over a threshold of 5 (-2) m $s^{-1}$ corresponding to the 65$^{th}$ percentile of the northward (southward) alongshore wind stress. The cumulative alongshore wind stress was used as a proxy for the intensity of wind-driven upwelling (downwelling) event. Additionally, the frequency and cumulative duration of these events were determined by counting the number of days that each event exceeded and sustained the specified threshold levels.

to which remote forcings from climatic modes are related to changes in local winds. First, we explored the influence of climate modes on interannual timescales. The coast of central Chile experiences changes in environmental conditions during El Niño through both oceanic and atmospheric teleconnections (Pizarro et al., 2002; Cai et al., 2020). Recently, a mode of variability linearly independent of El Niño, named Chile El Niño, was also shown to influence SST variability off Central Chile (Xue et al., 2020). Influences from the Southern Ocean are also possible particularly through the South Annular Mode (SAM) (Garreaud et al., 2019; Aguirre et al., 2021). Over the period of the present study, however, we did not find any significant relationship between along-shore wind stress, diatom abundance and these climate modes based on a multilinear model (not shown), and this is consistent with no observations of extreme climate events during this period. Therefore, we focus on decadal timescales, considering the existence of threshold values for wind stress to trigger a specific biological response. Thus, we now examine the low-pass filtered alongshore wind stress ($\tau_y$) at the PLV site (see blue line in Figure 1D) and compare this to the PDO index (see black continuous line in Figure 1D). These two time series were highly negatively correlated (r=-0.75 p=0.00) over the period 1982-2017. This suggests that over the study period (2000-2009), concomitant with a negative phase of the PDO, the low-frequency wind stress at PLV exhibits a steady increase, reaching a peak of 0.026 N $m^{-2}$ in 2007 (See Figure 1D). We argue that the mean wind conditions reached in 2005 were favorable for the enhancement of phytoplankton biomass. To assess the slow wind-driven changes on biomass, we calculated the low-pass filtered monthly surface Chl-a at the PLV site over the period 2000–2017 as a proxy for phytoplankton biomass. The concentration of Chl-a clearly increased at PLV from 2000 until 2007 in phase with the decadal fluctuations of the alongshore wind stress (with a correlation coefficient of r=0.96; p=0.00). With such variable winds in this region, it is worth inspecting low-frequency changes in high-frequency winds (intra-seasonal scale), which can result from the modulation of

TABLE 4 Thermal upwelling index based on the synoptic daily Sea Surface Temperature (SST) anomalies in Tongoy Bay.

| Sea Surface temperature (SST) index | | | | | | | |
|---|---|---|---|---|---|---|---|
| Period | | Cooling events | | | Warming events | | |
| | | N° (#) | Cumulative duration $D_e$ (days) | Cumulative Intensity (°C) | N° (#) | Cumulative duration $D_e$ (days) | Cumulative intensity (°C) |
| 2000 - 2004 | Fall - winter | 44 | 540 | 10.4 | 22 | 292 | 4 |
| | Spring - summer | 50 | 587 | 11.3 | 8 | 79 | 2.1 |
| | Total | 94 | 1127 | 21.7 | 30 | 371 | 6.1 |
| 2005 - 2009 | Fall - winter | 61 | 570 | 13.2 | 15 | 173 | 3 |
| | Spring - summer | 61 | 542 | 12 | 2 | 28 | 0.3 |
| | Total | 122 | 1112 | 25.2 | 17 | 201 | 3.4 |

Within each study period (1 and 2) and season, the intensity of the cold and warm synoptic SST anomalies triggered by upwelling or downwelling favorable alongshore winds, respectively, was quantified in terms of temporal extension $D_e$ (days) and cumulative mean intensity (°C days) of cooling or warming events. Upwelling (downwelling) favorable winds were identified as episodes when southerly (northerly) alongshore wind exceeded and remained above a threshold of 5 (-2) m $s^{-1}$ corresponding to the 65$^{th}$ percentile of the northward (southward) alongshore wind stress. The duration of each cooling (warming) event was calculated as the number of days elapsed between the onset of a temperature drop (rise) and the subsequent zero-crossing as temperature anomalies returned to positive (negative) values.

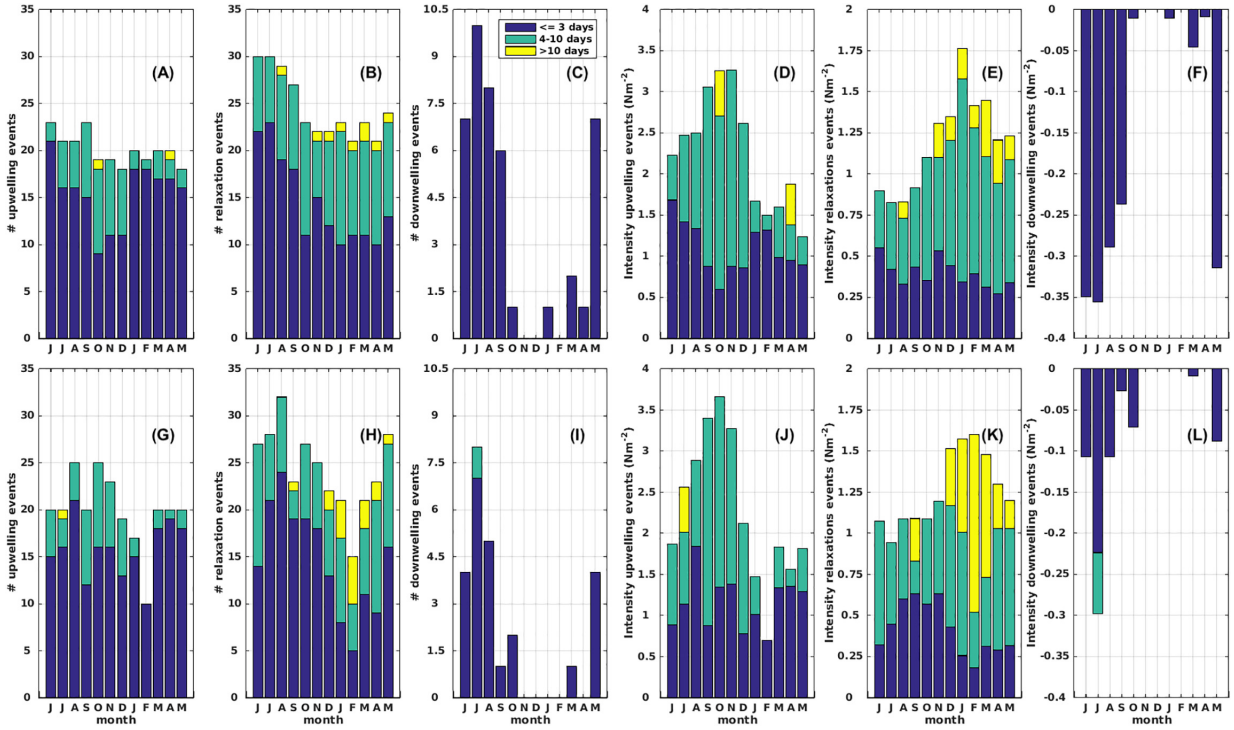


FIGURE 9
Annual cycles of cumulative number (#) and intensity (N $m^{-2}$) of upwelling, downwelling and relaxation events. Cumulative number and intensity of events in the upper panels corresponded to period 1 (January 2000 to December 2004) [**(A–C)** and **(D–F)**, respectively] whereas lower panels corresponded to period 2 (January 2005 to December 2009) [**(G–I)** and **(J–L)**, respectively]. Upwelling, downwelling and relaxation events are additionally classified by temporal extension into three categories: short (<= 3 days), medium (4–10 days), and long events (>10 days).

extratropical storms by low-frequency changes in the South Pacific Anticyclone (Renault et al., 2012). The time series of the low-pass filtered running variance of the intra-seasonal anomalies of the meridional wind stress in the PLV is displayed in Figure 1D (black dashed line). This index (low-pass $\tau_y$ ISA) measures how high-frequency variations in alongshore winds vary in amplitude at low-frequencies, and interestingly exhibits a "seesaw" pattern over the study period, with a reversal from positive to negative values in 2005. Such variations were unprecedented over the period 1982-2017. Note that low-frequency variations in high-frequency wind stress activity in PLV at 30°S do not correlate with those within the climatological area of the SEP Anticyclone (see Figure 1C).

# 5 Discussion

## 5.1 Abundance of diatoms and dinoflagellates and associated driving factors

In this paper, we show that during the period 2000-2009 microphytoplankton abundance and diversity in Tongoy Bay experienced a sharp change after 2005. These changes consisted of an abrupt increase in abundance of diatoms and dinoflagellates, and more frequent productive pulses associated with increased diversity and evenness of assemblages after 2005. In contrast, the period 2000-2004 was characterized by lower abundances of these two broad taxonomic groups associated with lower diversity and evenness and accompanied by several episodes of blooms dominated by harmful species. These changes are shown to be concomitant with the transition phase of the PDO from positive (warm) to negative (cold) between late-2004 and early-2005 (Ancapichún and Garcés, 2015), which is associated with an increase in the mean along-shore wind stress post 2005. Over the more extended period 1982-2017, low-pass filtered monthly alongshore wind stress at the PLV site also exhibited variations related to the PDO index, indicating that upwelling favorable winds increased during the cooler PDO phase (See Figure 1D). This is consistent with previous studies suggesting a relationship between time-space variations in the Southeast East Pacific Subtropical Anticyclone and the Pacific inter-decadal oscillation, which ultimately modulate the alongshore wind stress of north-central Chile (Ancapichún and Garcés-Vargas, 2015; Aguirre et al., 2018).

Our data also provide evidence that microphytoplankton activity was non-linearly related to upwelling favorable wind stress over the period 2000-2009 (See Figure 11). This non-linear relationship stems from the threshold level of wind stress, which, starting in 2005, triggered a significant increase in abundances of diatoms and dinoflagellates, but it can also be observed over the period after 2004, which involves higher-frequency variability timescales. The microphytoplankton abundances versus along-shore wind stress is consistent with the dome-shaped relationship (Botsford et al., 2003) as suggested by the parabolic fit (see black curve in Figures 11B, D) accounting for significantly larger

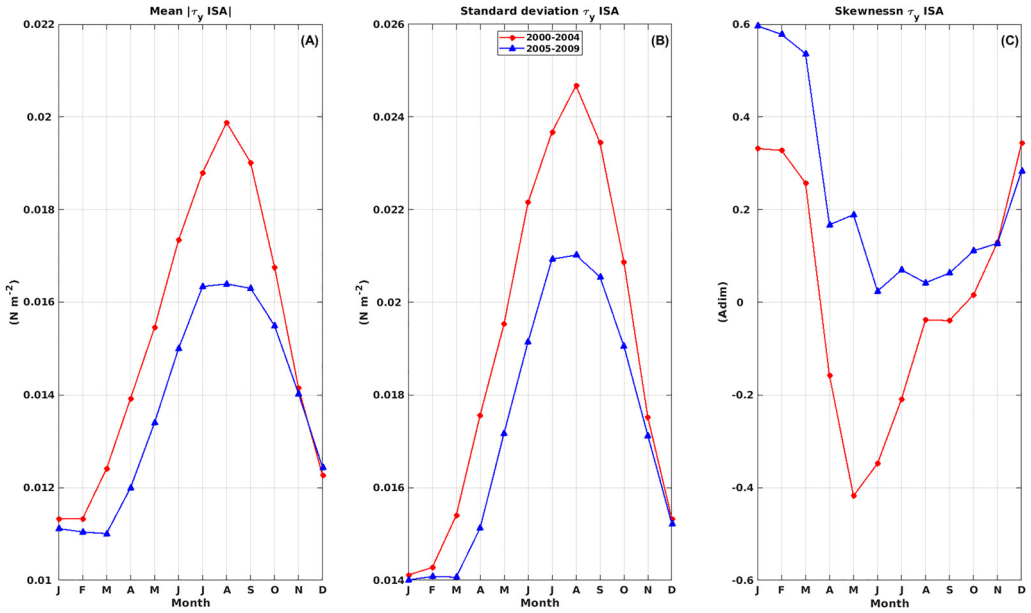


FIGURE 10
Monthly mean of the 3-month running **(A)** mean absolute value, **(B)** standard deviation and **(C)** skewness of alongshore wind stress ($\tau_y$) Intra-Seasonal Anomaly (ISA). January 2000 to December 2004 (red) and January 2005 to December 2009 (blue).

explained variance than the linear fit. Specifically for diatoms and dinoflagellates, the coefficient of determination ($R^2$) for the period 2005-2009 reaches values of 0.045 and 0.029 for the quadratic fit, versus values of 0.015 and 0.006 for the linear fit, respectively (See Supplementary Table S3). The bootstrapping method provided support for the dome-shape response of diatoms and dinoflagellates to the wind stress after 2005, where average abundances of diatoms and dinoflagellates were maximized at intermediate alongshore wind stress, reaching values of 10.4 x $10^5$ cell $L^{-1}$ and 928 cell $L^{-1}$, respectively (See Figures 11B, D and Supplementary Table S3). Over the period 2000-2004, the quadratic fit also better modeled the relationship between diatom abundance and along-shore wind stress than the linear fit, however, the relationships do not show a clear dome-shape compared with period post-2005. These scatter diagrams also showed that surface temperatures were most variable over the intermediate wind stress range, and were cooler at the lowest and highest winds stress levels, suggesting a higher intermittence between cooling and warming when medium wind stress prevailed (See Figure 11). This suggests the existence of a critical value in mean long-shore wind stress that maximizes plankton productivity in the coastal system of Tongoy Bay, a finding that is consistent with the observations of Stone et al. (2020) for the California upwelling ecosystem. However, Tongoy Bay behaves more like an upwelling shadow rather than a coastal system directly exposed to upwelling (Moraga-Opazo et al., 2011), implying that more complex physical factors are involved. Here we show that high-frequency components of the coastal winds could be at play to explain the non-linear relationship between wind stress and microphytoplankton productivity. We evidenced low-frequency variations (decadal scale) in the high-frequency along-shore wind stress (i.e. intra-seasonal scale), which manifests as a decrease after 2005 over our study period (See Figure 1 black dashed line). In other words, concomitant with the cold phase of the PDO observed after 2005 (See Figure 1D), the mean wind stress at PLV reached a maximum threshold value of 0.026 N $m^{-2}$ (between 2006 and 2008) when the intra-seasonal wind stress showed a weaker activity compared to the period prior to 2005 (negative trend). High-frequency winds can in particular have a role on how water mass properties are advected into the bay through instability processes (eddies, filaments) (Moraga-Opazo et al., 2011), which adds to the non-linear nature of the circulation. Overall, our data suggest that during the period between 2005 and 2009 the coupling of atmospheric and oceanic processes on the low-frequency time scale support the conceptual view of an "optimal wind window" for microphytoplankton productivity in Tongoy Bay and adds a potentially important factor to this concept: low-frequency changes in high-frequency wind activity.

A non-linear relationship between wind and phytoplankton biomass has also been highlighted by García-Reyes et al. (2014) for the Northern California upwelling system. These authors showed that the relationships between SST at an event scale, the nutrient upwelling index NUI (which quantifies the entrainment of cold water and nutrients to the surface layer) and Chl-a concentration, followed a dome-shaped function, suggesting that the highest levels of primary and secondary productivity occurred during moderate upwelling conditions. Other studies have indicated that the dome-shaped relationship with upwelling strength extends across trophic levels from phytoplankton to zooplankton and secondary consumers such as fish (Ruzicka et al., 2016). To further understand the mechanisms underlying this non-linear dome-shaped relationship, we analyzed the change in the annual cycle of the $\tau_y$ ISA between the two periods (see Figure 10), considering that the intra-seasonal timescales of variability are particularly relevant for blooms of microphytoplankton. Intra-seasonal wind stress was lower and less

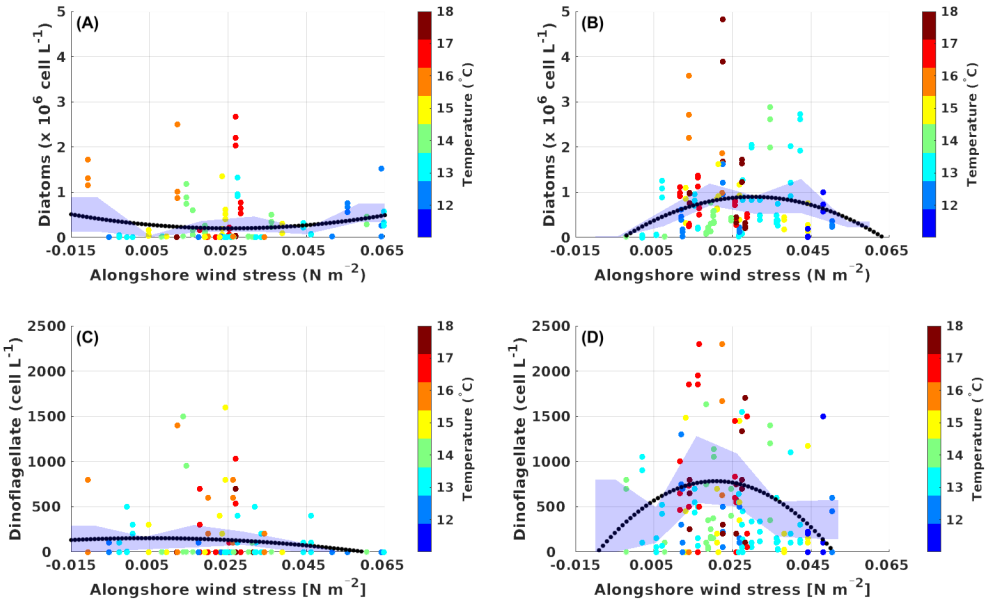


FIGURE 11
Relationship between alongshore wind stress, microphytoplankton communities (diatom and dinoflagellate), and sea surface temperature for period 1 (July 2002 to December 2004) in panels **(A, C)**, and for period 2 (January 2005 to December 2009) in panels **(B, D)**. The black dotted curve represents the quadratic fit of the relationship between alongshore wind stress and microphytoplankton communities. The blue shading indicates the 95% confidence interval for each of the microphytoplankton communities and for each period. SST and alongshore wind stress data were obtained from the ERA-5 reanalysis product. Diatom and dinoflagellate abundance data is based on *in situ* measurements collected in the upper water column (0- 10 m depth) at stations T4, T5, T11 in Tongoy Bay (See Figure 2). Mean microphytoplankton concentration against alongshore wind stress bins and 95% confidence intervals were calculated following Stone et al. (2020) using the bootstrapping method (Efron and Tibshirani, 1994). The bootstrap method involves resampling the original dataset with replacement to create multiple new datasets of the same size as the original. This approach entails drawing random samples from the data, allowing for duplicates, and repeating this process many times. For each resampled dataset of diatom or dinoflagellate abundance by wind stress bins between 0.01 - 0.06 N $m^{-2}$; the mean microphytoplankton abundance and confidence intervals were estimated using 10,000 iterations.

variable during period 2 than period 1 (See Figures 10A, B). Lower amplitude synoptic wind speeds were associated with a positive skewness of $\tau_y$ ISA (i.e. higher activity in upwelling-favorable pulses) throughout the annual cycle during period 2 (See Figure 10C), suggesting that oceanographic conditions in the upper water column could have been characterized by reduced mixing (i.e. higher water column stability) that improved nutrient uptake by photosynthetic diatoms and dinoflagellates and in turn, improved the food availability to heterotrophic species. By contrast, a higher and more variable mean $\tau_y$ ISA and negative skewness (i.e. higher activity toward southward wind anomalies) in the late summer-winter seasons (March-September) (See Figure 10C), could be associated with enhanced mixing because more intense high-frequency wind variations can more effectively produce current shears in the surface layer and thus enhance turbulence.

The notable changes in the intra-seasonal alongshore wind phenology explain the observed differences in annual cycles of microphytoplankton, where period 2 was characterized by multiple peaks of diatoms and dinoflagellates throughout the year, probably fuelled by recurrent nutrient fertilization pulses (see Figures 5, 6). However, these recurrent upwelling pulses should be followed by periods of wind relaxation over time scales on the order of microphytoplankton blooms in order to maximize abundances (Botsford et al., 2006). In this regard, our analyses of annual cycles of upwelling, relaxation and downwelling events – when separated by temporal extension (≤ 3 days, 4 - 10 days, > 10 days) – showed that during period 2 the following processes occurred: (i) cumulative upwelling intensity reached higher values in September and October coinciding with maxima of diatom abundance, (ii) longer relaxation periods (> 10 days) during the spring and summer seasons, but particularly during summer (January to March) when dinoflagellates reached the highest abundances; and iii) notable decreases in downwelling events, especially during the period between November and February (See Figure 9). These observations suggest that underlying mechanisms driving the dome shaped phytoplankton-wind relationship after 2005 may be explained by two combined processes: i) increase in the mean alongshore wind during a cold PDO phase reaching an optimal threshold associated with higher (but less variable) monthly means of alongshore wind stress, Ekman transport, Ekman pumping and total transport, and a reduction in frequency, duration and intensity of the warming episodes; and ii) changes in the intra-seasonal wind phenology characterized by lower intensity, relaxation periods longer than 10 days during spring-summer, and fewer downwelling episodes. All of these processes favored the growth of microphytoplankton within Tongoy Bay, likely due to higher nutrient availability and optimal uptake conditions, that is, an uplifted nitracline due to stronger winds enhancing nitrate concentration within the euphotic zone combined with overall reduced mixing rates due to less variable winds, which favors reduced dilution of micro-phytoplankton. On the other hand,

the lack of a dome-shape in the microphytoplankton-wind relationship during period 1 (2000-2004) suggests that the combined effects of a stronger intra-seasonal activity in the alongshore wind stress along with increased downwelling events could have triggered recurrent dilution processes of diatom and dinoflagellates assemblages. It has been recognized that the initiation of upwelling essentially "reset" the successional state of the system because upwelling typically represent a source of nutrients but a loss of organisms (Botford et al., 2003; Jacox et al., 2016). Thus, the relative degree of mixing derived from upwelling intensity versus duration of relaxation events, and fewer downwelling episodes, were critical factors underlying the dependence of productivity on wind in the Tongoy Bay.

In addition to inter-annual variability in the microphytoplankton abundances that are modulated by changes in the large-scale climatic phenomena and high frequency winds, we also detected marked seasonal variability in the biological response associated with the ocean-atmospheric interplay in Tongoy Bay. Our analyses of daily alongshore wind stress and thermal upwelling index of the synoptic daily sea surface temperature anomalies in Tongoy Bay showed that during spring and summer months (cold anomalies), the upwelling-favorable wind stress and offshore transport increased in frequency and amplitude in association with the southward seasonal displacement of the South East Pacific (SEP) subtropical anticyclone (Rahn, 2012). In contrast, during the autumn-winter months (warm anomalies) winds were alternated with periods of northerly downwelling-favorable winds associated with transient meteorological phenomena such as cyclonic frontal disturbances and coastal lows (Rutllant et al., 2004; Renault et al., 2009). Changes in the direction of winds triggered seasonal patterns in diatom and dinoflagellate abundances in Tongoy Bay, where the spring-summer season exhibited cell abundances one order of magnitude higher than observed in fall-winter. The seasonal variability of primary producers has been typically described for the central-southern area (30- 40°S) of the Humboldt current system (Daneri et al., 2000; Thiel et al., 2007; Montero et al., 2007; Jacob et al., 2018) where strong upwelling of cool nutrient-rich subsurface waters of equatorial origin show a more seasonal pattern compared with the non-seasonal trend exhibited in systems located further north (18°S–24°S), which, in turn, has been also associated with weak seasonality in chlorophyll-a concentrations (Thomas et al., 2001). An interesting point to note is that intra-seasonal wind variability is much less in the northern area (northward of 26°S, see Figure 3A of Monteiro et al., 2011), suggesting that changes in the intra-seasonal variability is not likely to be a key factor influencing phytoplankton productivity compared to areas located southward of 26°S. On the other hand, the coastal system off northern Chile has been described as a system with persistently low phytoplankton productivity in comparison with upwelling ecosystems located along the Humboldt Current System off southern Chile (Daneri et al., 2000 and cites therein) which contrast with our findings. We found that the surface Chl-a concentrations estimated from satellites during period 2 were higher (6.6 μg $L^{-1}$) than those estimated from satellites in recent reports for the coastal area off northern and central Chile during the period 2002- 2018 (Tornquist et al., 2024). On the other hand, diatom abundances (> 2 x $10^6$ cells $L^{-1}$) in this study were of a similar order of magnitude to diatom abundances measured at sites 18 miles off Concepción, one of the most productive coastal ecosystem of the Humboldt current system off Chile (Jacob et al., 2018). This suggests that primary productivity in Tongoy Bay may be maximized when optimal environmental conditions prevail. Our findings thus suggest that the interpretation of phytoplankton productivity and biomass in upwelling ecosystems requires analyses of winds over high-frequency (days to weeks) temporal scales (Jacob et al., 2011; García-Reyes et al., 2014).

## 5.2 On the role of the diversity of diatoms and dinoflagellates in Tongoy Bay

The elevated abundance of diatoms and dinoflagellate observed from 2005 onwards was accompanied by significant increases in the richness and evenness of both groups, and was associated with higher oxygenation levels and cooler temperatures in the first 15 m of the water column. This is highlighted by the increase in diversity and evenness (May 2005 for diatoms) occurring in the same period (May/June) as the elevated upper water oxygenation (positive anomaly of 0.79 mg $L^{-1}$) post-2005 (See Figure 7D). This suggests that a more diverse and equitably distributed community promoted higher rates of photosynthesis in Tongoy Bay. Several studies have provided syntheses of the effects of alterations of biodiversity on ecosystem functioning and concluded that biodiversity has a major role in sustaining both the productivity and stability of ecosystems (Cardinale et al., 2012; Tilman et al., 2014; Otero et al., 2020). Moreover, several studies conducted in both fresh and marine waters have concluded that increased diversity enhances resource use efficiency (RUE, i.e., an ecological index that measures the proportion of supplied resources turned into new biomass; Hodapp et al., 2019) for primary producers (Ptacnik et al., 2008; Olli et al., 2014; Otero et al., 2020), supporting the hypothesis that when biodiversity increases, the rate of ecosystem functioning also increases (Sala et al., 1996). The biological basis of this hypothesis could be niche complementarity (Tilman, 1999), positive interactions among species (Cardinale et al., 2002; Bruno et al., 2003) and a greater capacity of certain species to utilize resources (Otero et al., 2020). These concepts refer to diverse communities making differential use of resources resulting in higher functioning rates and positive interactions such as symbiosis increasing production capacity, while certain functional characteristics allow some species to make greater use of resources.

Studies carried out off the Galician coast in northern Spain using a 28-year time-series of phytoplankton diversity data showed that biodiversity was the principal factor modulating resource use compared to environmental factors, such as temperature and upwelling intensity, and concluded that biodiversity is important for maintaining planktonic production, highlighting in turn the relevance of complementary niche effects (Otero et al., 2020). In general, our findings showed that both richness and evenness indices were higher during period 2 than period 1, suggesting that the number of diatom and dinoflagellate species post-2005 was important in maintaining high total abundances leading to the hypothesis of the relevance of complementarity effects. The higher evenness index allowed us to hypothesize that assemblages were dominated by a high diversity of diatom and dinoflagellate species

with functional traits that exploit resources in a complementary manner. In contrast, period 1 exhibited a lower evenness trend suggesting that selection effect took place, leading to assemblages being dominated by diatom and dinoflagellate species with more specific functional traits that improved their competitive abilities. The latter was reflected in some blooms being exclusively or partially dominated by diatom species such as *Pseudo-nitzschia australis*, *Pseudo-nitzschia pungens, Detonula pumila*, *Skeletonema costatum*, *Asterionellopsis glacialis* with dinoflagellate blooms dominated by *Prorocentrum gracile*. Interestingly, and perhaps crucially, some of the dominant diatom species such *Detonula pumila* and *Pseudo-nitzschia australis* decreased their relative contribution to total abundance by one order of magnitude when the oceanographic regime shifted post-2005 (i.e. higher Ekman pumping and longer relaxation episodes post-upwelling). This suggests that nutrient inputs modified the community composition (Dittrich et al., 2023), with implications perhaps for some potentially harmful species.

Diatoms such as *Pseudo-nitzschia australis* and *Pseudo-nitzschia pungens* have been associated with amnesic shellfish poisoning (ASP) in some regions of the world (Garrison et al., 1992; Rhodes et al., 2003; Trainer et al., 2012; Bates et al., 2018; Sauvey et al., 2023) with the former species being one of the most important producers of the causative agent, domoic acid (Alvarez et al., 2009). Domoic acid concentrations have in the past exceeded the regulatory limit (20 mg $kg^{-1}$) leading to the banning of shellfish harvesting from wild populations in some bays in northern Chile (Alvarez et al., 2020). Notably, the high abundances reached by *Pseudo-nitzschia australis* blooms (> 2 x $10^6$ cells $L^{-1}$) in Tongoy Bay (January 2003 and February 2004, this study) were similar to those reached during a bloom in Bahía Inglesa in northern Chile in November 2006 (1.6 x $10^6$ cells $L^{-1}$), where elevated domoic acid concentrations (103 mg $kg^{-1}$ wet weight) were associated with dominance by the diatom *Pseudo-nitzschia spp* (80% of the total phytoplankton biomass) that affected the harvesting of scallops from aquaculture sites (Díaz et al., 2019). The native scallop *Argopecten purpuratus* is subjected to aquaculture practices in Tongoy Bay supporting production that exceeds 3200 tons per year (Bakit et al., 2022; SERNAPESCA, 2022). The findings of the present study are relevant here because of the need for this bivalve to cope with environmental conditions induced by upwelling, such as colder, lower pH and hypoxic waters associated with persistent upwelling episodes (Ramajo et al., 2020). Furthermore, increasing warming of the ocean surface and associated marine heatwaves could intensify abundance of *Pseudo-nitzschia* and the associated outbreaks of domoic acid production (Collins et al., 2019) that threaten the harvesting of commercial species (Trainer et al., 2020).

Analyses of the historical record of large-scale harmful algal blooms caused by *Pseudo-nitzschia* have demonstrated that these events tend to occur during periods of anomalously warm ocean conditions associated with the positive phase of the Pacific Decadal Oscillation (PDO), and with conditions observed during El Niño and marine heatwaves (McCabe et al., 2016; McKibben et al., 2017). Our results are consistent with this as we observed higher and lower *Pseudo-nitzschia* abundances during the warm and cold phases of the PDO, respectively, associated with changes in the frequency, duration and intensity of warming and cooling events (See Table 4). This suggests that the period between 2005 and 2009 may have provided a "temporary environmental refuge" to *Argopecten purpuratus* resulting from higher food availability, higher oxygenation levels and lower abundance of harmful phytoplankton in its diet. Our observations provide a potential avenue for further research, but a more extended time series of phytoplankton in Tongoy Bay would be required to confirm such a relationship with PDO-induced wind changes. Our future plan would be to experiment with the application of a long-term biogeochemical model to overcome limitations in the present data set.

## 6 Concluding remarks

Overall, our analysis of an unprecedented data set provides evidence of the interaction – over various timescales – between environmental conditions and microphytoplankton abundances, species composition and diversity in a typical upwelling shadow system of the Southern Hemisphere EBUS. Our data suggest that over the period 2000-2009, microphytoplankton activity was non-linearly related to upwelling favorable wind stress driven by the PDO in combination with reduced high frequency winds (synoptic frequency band). Elevated microphytoplankton abundances and more frequent blooms were observed from 2005 onwards, and this was accompanied by a significant increase in richness and evenness of both diatom and dinoflagellate groups, and in water column oxygenation. We highlight the role of decadal oscillations in the variability of harmful algae blooms observed in Tongoy Bay (e.g. *Pseudo-nitzschia australis*), with implications for frequency and toxicity of these blooms under a scenario of ocean warming. Because of the local socio-economic importance of *Argopecten purpuratus* aquaculture and local fisheries, future research on productivity in Tongoy Bay should focus on modeling the key role of intra-seasonal winds under the changing upwelling conditions related to the PDO.

## Data availability statement

The data analyzed in this study was obtained from SERNAPESCA databases. Requests to access these datasets should be directed to SERNAPESCA.

## Ethics statement

The manuscript presents research on animals that do not require ethical approval for their study.

## Author contributions

BJ: Conceptualization, Investigation, Methodology, Software, Supervision, Validation, Writing – original draft, Writing – review &

editing, Formal analysis, Funding acquisition. OA: Conceptualization, Investigation, Methodology, Software, Writing – review & editing, Writing – original draft, Funding acquisition, Formal analysis, Supervision. BD: Conceptualization, Investigation, Methodology, Validation, Writing – original draft, Writing – review & editing, Funding acquisition, Formal analysis. MV: Conceptualization, Formal analysis, Methodology, Software, Writing – review & editing. GAA: Data curation, Formal analysis, Investigation, Methodology, Resources, Writing – original draft, Writing – review & editing. CM: Formal analysis, Methodology, Software, Writing – review & editing. DC: Formal analysis, Writing – original draft. EU: Conceptualization, Data curation, Formal analysis, Funding acquisition, Investigation, Methodology, Resources, Validation, Writing – original draft. BY: Conceptualization, Data curation, Funding acquisition, Methodology, Resources, Writing – review & editing.

## Funding

The author(s) declare financial support was received for the research, authorship, and/or publication of this article. This research was funded by FONDEF DOI 1056, Ostimar S.A, FIP N° 2007-20. BJ was funded by ANID Regional 2020-R20F0002 (CIEP). BD acknowledges support from ANID (Concurso de Fortalecimiento al Desarrollo Científico de Centros Regionales 2020-R20F0008-CEAZA, Centro de Investigación Oceanográfica en el Pacífico Sur-Oriental COPAS COASTAL FB210021, and Fondecyt Regular N°1231174) and from the EU H2020 Future Mares project (Theme LC-CLA-06-2019, Grant agreement No 869300). OA acknowledges the support from FONDECYT project 11190999.

## Conflict of interest

The authors declare that the research was conducted in the absence of any commercial or financial relationships that could be construed as a potential conflict of interest.

## Publisher's note



## Supplementary material

The Supplementary Material for this article can be found online at: https://www.frontiersin.org/articles/10.3389/fmars.2024.1434007/full#supplementary-material

## References

Aguirre, C., Flores-Aqueveque, V., Vilches, P., Vásquez, A., Rutllant, J. A., and Garreaud, R. (2021). Recent changes in the low-level jet along the subtropical west coast of south america. *Atmosphere* 12, 465. doi: 10.3390/atmos12040465

Aguirre, C., García-Loyola, S., Testa, G., Silva, D., and Farías, L. (2018). Insight into anthropogenic forcing on coastal upwelling off south-central Chile. *Elementa: Sci. Anthropocene* 6. doi: 10.1525/elementa.314

Álvarez, G., Uribe, E., Quijano-Scheggia, S., López-Rivera, A., Mariño, C., and Blanco, J. (2009). Domoic acid production by *Pseudo-nitzschia australis* and *Pseudo-nitzschia calliantha* isolated from North Chile. *Harmful Algae* 8, 938–945. doi: 10.1016/j.hal.2009.05.005

Álvarez, G., Rengel, J., Araya, M., Álvarez, F., Pino, R., Uribe, E., et al. (2020). Rapid domoic acid depuration in the scallop *argopecten purpuratus* and its transfer from the digestive gland to other organs. *Toxins* 12, 698. doi: 10.3390/toxins12110698

Ancapichún, S., and Garcés-Vargas, J. (2015). Variability of the Southeast Pacific Subtropical Anticyclone and its impact on sea surface temperature off north-central Chile. *Cienc. Mar.* 41, 1–20. doi: 10.7773/cm.v41i1.2338

Antoine, D., Morel, A., Gordon, H. R., Banzon, V. F., and Evans, R. H. (2005). Bridging ocean color observations of the 1980s and 2000s in search of long-term trends. *J. Geophys. Res.* 110. doi: 10.1029/2004jc002620

Bakit, J., Álvarez, G., Díaz, P. A., Uribe, E., Sfeir, R., Villasante, S., et al. (2022). Disentangling environmental, economic, and technological factors driving scallop (*Argopecten purpuratus*) aquaculture in Chile. *Fishes* 7, 380. doi: 10.3390/fishes7060380

Bakun, A. (1973). "Coastal upwelling indices, west coast of North America 1946-71," in *U.S. Dept. of commerce, NOAA tech. Rep*, Unites States. 103p. NMFS SSRF-671.

Bates, S. S., Hubbard, K. A., Lundholm, N., Montresor, M., and Leaw, C. P. (2018). *Pseudo-nitzschia*, *Nitzschia*, and domoic acid: New research since 2011. *Harmful Algae* 79, 3–43. doi: 10.1016/j.hal.2018.06.001

Behrenfeld, M. J., O'Malley, R. T., Siegel, D. A., McClain, C. R., Sarmiento, J. L., Feldman, G. C., et al. (2006). Climate-driven trends in contemporary ocean productivity. *Nature* 444, 752–755. doi: 10.1038/nature05317

Benoiston, A. S., Ibarbalz, F. M., Bittner, L., Guidi, L., Jahn, O., Dutkiewicz, S., et al. (2017). The evolution of diatoms and their biogeochemical functions. *Philos. Trans. R. Soc. B: Biol. Sci.* 372, 20160397. doi: 10.1098/rstb.2016.0397

Blanchard, J. L., Jennings, S., Holmes, R., Harle, J., Merino, G., Allen, J. I., et al. (2012). Potential consequences of climate change for primary production and fish production in large marine ecosystems. *Philos. Trans. R. Soc. B: Biol. Sci.* 367, 2979–2989. doi: 10.1098/rstb.2012.0231

Blanco, J. L., Carr, M., Thomas, A. C., and Strub, P. T. (2002). Hydrographic conditions off northern Chile during the 1996–1998 La Niña and El Niño events. *J.-Geophys.-Res.* 107. doi: 10.1029/2001jc001002

Botsford, L. W., Lawrence, C. A., Dever, E. P., Hastings, A., and Largier, J. (2003). Wind strength and biological productivity in upwelling systems: an idealized study. *Fisheries Oceanography* 12, 245–259. doi: 10.1046/j.1365-2419.2003.00265.x

Botsford, L. W., Lawrence, C. A., Dever, E. P., Hastings, A., and Largier, J. (2006). Effects of variable winds on biological productivity on continental shelves in coastal upwelling systems. *Deep Sea Res. Part II: Topical Stud. Oceanography* 53, 3116–3140. doi: 10.1016/j.dsr2.2006.07.011

Boyce, D. G., Lewis, M. R., and Worm, B. (2010). Global phytoplankton decline over the past century. *Nature* 466, 591–596. doi: 10.1038/nature09268

Bravo, L., Ramos, M., Astudillo, O., Dewitte, B., and Goubanova, K. (2016). Seasonal variability of the Ekman transport and pumping in the upwelling system off central-northern Chile (∼ 30°S) based on a high-resolution atmospheric regional model (WRF). *Ocean Sci.* 12, 1049–1065. doi: 10.5194/os-12-1049-2016

Brown, A. R., Lilley, M., Shutler, J., Lowe, C., Artioli, Y., Torres, R., et al. (2020). Assessing risks and mitigating impacts of harmful algal blooms on mariculture and marine fisheries. *Rev. Aquaculture* 12, 1663–1688. doi: 10.1111/raq.12403

Bruno, J. F., Stachowicz, J. J., and Bertness, M. D. (2003). Inclusion of facilitation into ecological theory. *Trends Ecol. Evol.* 18, 119–125. doi: 10.1016/s0169-5347(02)00045-9

Cai, W., McPhaden, M. J., Grimm, A. M., Rodrigues, R. R., Taschetto, A. S., Garreaud, R. D., et al. (2020). Climate impacts of the el niño–southern oscillation on south america. *Nat. Rev. Earth Environ.* 1, 215–231. doi: 10.1038/s43017-020-0040-3

Cardinale, B. J., Duffy, J. E., Gonzalez, A., Hooper, D. U., Perrings, C., Venail, P., et al. (2012). Biodiversity loss and its impact on humanity. *Nature* 486, 59–67. doi: 10.1038/nature11148

Cardinale, B. J., Palmer, M. A., and Collins, S. L. (2002). Species diversity enhances ecosystem functioning through interspecific facilitation. *Nature* 415, 426–429. doi: 10.1038/415426a

Carr, M., Strub, P. T., Thomas, A. C., and Blanco, J. L. (2002). Evolution of 1996–1999 La Niña and El Niño conditions off the western coast of South America: A remote sensing perspective. *J. Geophys. Res.* 107. doi: 10.1029/2001jc001183

Chavez, F. P., Messié, M., and Pennington, J. T. (2011). Marine primary production in relation to climate variability and change. *Annu. Rev. Mar. Sci.* 3, 227–260. doi: 10.1146/annurev.marine.010908.163917

Chiba, S., Batten, S., Sasaoka, K., Sasai, Y., and Sugisaki, H. (2012). Influence of the Pacific Decadal Oscillation on phytoplankton phenology and community structure in the western North Pacific. *Geophysical Res. Lett.* 39. doi: 10.1029/2012gl052912

Chin, T. M., Vazquez-Cuervo, J., and Armstrong, E. M. (2017). A multi-scale high-resolution analysis of global sea surface temperature. *Remote Sens. Environ.* 200, 154–169. doi: 10.1016/j.rse.2017.07.029

Collins, M., Sutherland, M., Bouwer, L., Cheong, S.-M., Frölicher, T., Combes, H., et al. (2019). "Extremes, abrupt changes and managing risk," in eds H.-O. Pörtner, D.C. Roberts, V. Masson-Delmotte, P. Zhai, M. Tignor, E. Poloczanska, et al. *IPCC Special Report on theOcean and Cryosphere in a Changing Climate*, (in press). Available at: https://www.ipcc.ch/srocc/chapter/chapter-6/ (accessed November 29, 2019).

Crawford, D. W., Cefarelli, A. O., Wrohan, I. A., Wyatt, S. N., and Varela, D. E. (2018). Spatial patterns in abundance, taxonomic composition and carbon biomass of nano- and microphytoplankton in Subarctic and Arctic Seas. *Prog. Oceanography* 162, 132–159. doi: 10.1016/j.pocean.2018.01.006

Cury, P., and Roy, C. (1989). Optimal environmental window and pelagic fish recruitment success in upwelling areas. *Can. J. Fish. Aquat. Sci.* 46, 670–680. doi: 10.1139/f89-086

Daneri, G., Dellarossa, V., Quiñones, R., Jacob, B., Montero, P., and Ulloa, O. (2000). Primary production and community respiration in the Humboldt Current System off Chile and associated oceanic areas. *Mar. Ecol. Prog. Ser.* 197, 41–49. doi: 10.3354/meps197041

Dewitte, B., Illig, S., Renault, L., Goubanova, K., Takahashi, K., GushChina, D., et al. (2011). Modes of covariability between sea surface temperature and wind stress intraseasonal anomalies along the coast of Peru from satellite observations, (2000–2008). *J. Geophys. Res.* 116. doi: 10.1029/2010jc006495

Díaz, P. A., and Álvarez, G. (2023). Effects of microalgal blooms on aquaculture and fisheries. *Fishes* 8. doi: 10.3390/fishes8090461

Díaz, P. A., Álvarez, G., Varela, D., Pérez-Santos, I., Díaz, M., Molinet, C., et al. (2019). Impacts of harmful algal blooms on the aquaculture industry: Chile as a case study. *pip* 6, 39–50. doi: 10.1127/pip/2019/0081

Díaz, P. A., Pérez-Santos, I., Basti, L., Garreaud, R., Pinilla, E., Barrera, F., et al. (2023). The impact of local and climate change drivers on the formation, dynamics, and potential recurrence of a massive fish-killing microalgal bloom in Patagonian fjord. *Sci. Total Environ.* 865, 161288. doi: 10.1016/j.scitotenv.2022.161288

Dittrich, J., Dias, J. D., de Paula, A. C. M., and Padial, A. A. (2023). Experimental nutrient enrichment increases plankton taxonomic and functional richness and promotes species dominance overtime. *Hydrobiologia* 850, 4029–4048. doi: 10.1007/s10750-023-05285-5

Efron, B., and Tibshirani, R. (1994). *An introduction to the bootstrap* (New York: Chapman and Hall).

Elferink, S., John, U., Neuhaus, S., and Wohlrab, S. (2020). Functional genomics differentiate inherent and environmentally influenced traits in dinoflagellate and diatom communities. *Microorganisms* 8, 567. doi: 10.3390/microorganisms8040567

European Union-Copernicus Marine Service (2022). *Global ocean colour (Copernicus-globColour), bio-geo-chemical, L4 (monthly and interpolated) from satellite observations, (1997-ongoing)*. doi: 10.48670/MOI-00281

Falkowski, P. G. (2012). Ocean science: the power of plankton. *Nature* 483, S17–S20. doi: 10.1038/483S17a

Falkowski, P. G., Barber, R. T., and Smetacek, V. (1998). Biogeochemical controls and feedbacks on ocean primary production. *Science* 281, 200–206. doi: 10.1126/science.281.5374.200

Falkowski, P. G., Fenchel, T., and Delong, E. F. (2008). The microbial engines that drive earth's biogeochemical cycles. *Science* 320, 1034–1039. doi: 10.1126/science.1153213

Field, C. B., Behrenfeld, M. J., Randerson, J. T., and Falkowski, P. (1998). Primary production of the biosphere: integrating terrestrial and oceanic components. *Science* 281, 237–240. doi: 10.1126/science.281.5374.237

Flynn, K. J., Mitra, A., Anestis, K., Anschütz, A. A., Calbet, A., Ferreira, G. D., et al. (2019). Mixotrophic protists and a new paradigm for marine ecology: Where does plankton research go now? *J. Plankton Res.* 41, 375–391. doi: 10.1093/plankt/fbz026

Fu, W., Randerson, J. T., and Moore, J. K. (2016). Climate change impacts on net primary production (NPP) and export production (EP) regulated by increasing stratification and phytoplankton community structure in the CMIP5 models. *Biogeosciences* 13, 5151–5170. doi: 10.5194/bg-13-5151-2016

García-Reyes, M., Largier, J. L., and Sydeman, W. J. (2014). Synoptic-scale upwelling indices and predictions of phyto- and zooplankton populations. *Prog. Oceanography* 120, 177–188. doi: 10.1016/j.pocean.2013.08.004

Garreaud, RenéD., and Battisti, D. S. (1999). Interannual (ENSO) and interdecadal (ENSO-like) variability in the southern hemisphere tropospheric circulation*. *J. Climate* 12, 2113–2123. doi: 10.1175/1520-0442(1999)012<2113:ieaiel>2.0.co;2

Garreaud, R. D., Boisier, J. P., Rondanelli, R., Montecinos, A., Sepúlveda, H. H., and Veloso-Aguila, D. (2019). The Central Chile Mega Drought, (2010–2018): A climate dynamics perspective. *Intl J. Climatology* 40, 421–439. doi: 10.1002/joc.6219

Garrison, D. L., Conrad, S. M., Eilers, P. P., and Waldron, E. M. (1992). Confirmation of domoic acid production by *Pseudonitzschia australis* (Bacillariophyceae) cultures. *J. Phycology* 28, 604–607. doi: 10.1111/j.0022-3646.1992.00604.x

Gill, A. (1982). *Atmosphere-ocean dynamics* (New York: Academic Press).

Glibert, P. M. (2016). Margalef revisited: A new phytoplankton mandala incorporating twelve dimensions, including nutritional physiology. *Harmful Algae* 55, 25–30. doi: 10.1016/j.hal.2016.01.008

Gómez, F. (2012a). A checklist and classification of living dinoflagellates (Dinoflagellata, Alveolata). *CICIMAR Oceánides* 27, 65–140. doi: 10.37543/oceanides.v27i1.111

Gómez, F. (2012b). A quantitative review of the lifestyle, habitat and trophic diversity of dinoflagellates (Dinoflagellata, Alveolata). *Syst. Biodivers* 10, 267–275. doi: 10.1080/14772000.2012.721021

Grattan, L. M., Holobaugh, S., and Morris, J. G.Jr. (2016). Harmful algal blooms and public health. *Harmful Algae* 57, 2–8. doi: 10.1016/j.hal.2016.05.003

Gregg, W. W., Casey, N. W., and McClain, C. R. (2005). Recent trends in global ocean chlorophyll. *Geophysical Res. Lett.* 32. doi: 10.1029/2004gl021808

Gruber, N., Lachkar, Z., Frenzel, H., Marchesiello, P., Münnich, M., McWilliams, J. C., et al. (2011). Eddy-induced reduction of biological production in eastern boundary upwelling systems. *Nat. Geosci.* 4, pp.787–pp.792. doi: 10.1038/ngeo1273

Guiry, M. D., and Guiry, G. M. (2024). *AlgaeBase* (Ireland: IrelandWorld-wide electronic publication, University of Galway). Available at: https://www.algaebase.org.

Hasle, G. R. (1978). "The inverted microscope method," in *Phytoplankton manual*. Ed. A. Sournia (UNESCO, Paris), 88–96.

Henson, S. A., Cael, B. B., Allen, S. R., and Dutkiewicz, S. (2021). Future phytoplankton diversity in a changing climate. *Nat. Commun.* 12. doi: 10.1038/s41467-021-25699-w

Hersbach, H., Bell, B., Berrisford, P., Hirahara, S., Horányi, A., Muñoz-Sabater, J., et al. (2020). The ERA5 global reanalysis. *Quart J. R. Meteoro Soc.* 146, 1999–2049. doi: 10.1002/qj.3803

Hickey, B. M., and Banas, N. S. (2008). Why is the Northern End of the California current system so productive? *Oceanography* 21, 90–107. doi: 10.5670/oceanog.2008.07

Hodapp, D., Hillebrand, H., and Striebel, M. (2019). Unifying" the concept of resource use efficiency in ecology. *Front. Ecol. Evol.* 6. doi: 10.3389/fevo.2018.00233

Isbell, F., Craven, D., Connolly, J., Loreau, M., Schmid, B., Beierkuhnlein, C., et al. (2015). Biodiversity increases the resistance of ecosystem productivity to climate extremes. *Nature* 526, 574–577. doi: 10.1038/nature15374

Ishida, H., John, U., Murray, S. A., Bhattacharya, D., and Chan, C. X. (2023). Developing model systems for dinoflagellates in the post-genomic era. *J. Phycology* 59, 799–808. doi: 10.1111/jpy.13386

Jacob, B., Daneri, G., Quiñones, R. A., and Sobarzo, M. (2011). Community metabolism, phytoplankton size structure and heterotrophic prokaryote production in a highly productive upwelling zone off northern Chile. *Mar. Ecol. Progr. Ser.* 430, 23–34. doi: 10.3354/meps09074

Jacob, B. G., Tapia, F. J., Quiñones, R. A., Montes, R., Sobarzo, M., Schneider, W., et al. (2018). Major changes in diatom abundance, productivity, and net community metabolism in a windier and dryer coastal climate in the southern Humboldt Current. *Prog. Oceanography* 168, 196–209. doi: 10.1016/j.pocean.2018.10.001

Jacox, M. G., Hazen, E. L., and Bograd, S. J. (2016). Optimal environmental conditions and anomalous ecosystem responses: constraining bottom-up controls of phytoplankton biomass in the california current system. *Sci. Rep.* 6. doi: 10.1038/srep27612

Khatiwala, S., Primeau, F., and Hall, T. (2009). Reconstruction of the history of anthropogenic $CO_2$ concentrations in the ocean. *Nature* 462, 346–349. doi: 10.1038/nature08526

Large, W., and Pond, S. (1981). Open ocean momentum flux measurements in moderate to strong winds. *J. Phys. Ocean.* 11, 324ogr–324336. doi: 10.1175/1520-0485(1981)011<0324:OOMFMI>2.0.CO;2

Largier, J. L., Lawrence, C. A., Roughan, M., Kaplan, D. M., Dever, E. P., Dorman, C. E., et al. (2006). WEST: A northern California study of the role of wind-driven transport in the productivity of coastal plankton communities. *Deep Sea Res. Part II: Topical Stud. Oceanography* 53, 2833–2849. doi: 10.1016/j.dsr2.2006.08.018

Lee, T., and McPhaden, M. J. (2010). Increasing intensity of El Niño in the central-equatorial Pacific. *Geophysical Res. Lett.* 37. doi: 10.1029/2010gl044007

Lindahl, O. (1986). "A dividable hose for phytoplankton sampling. Report of the working group on phytoplankton and management of their effects," in *International council for the exploration of the sea, C.M.1986/L.* (Sweden) 1926, Annex 1983.

Litchman, E., and Klausmeier, C. A. (2008). Trait-based community ecology of phytoplankton. *Annu. Rev. Ecol. Evol. Syst.* 39, 615–639. doi: 10.1146/annurev.ecolsys.39.110707.173549

Lovegrove, T. (1960). An improved form of sedimentation apparatus for use with an inverted microscope. *ICES J. Mar. Sci.* 25, 279–284. doi: 10.1093/icesjms/25.3.279

Lundholm, N., and Moestrup, Ø. (2006). "The biogeography of harmful algae," in *Ecology of harmful algae*. Eds. E. Granéli and J. T. Turner (Springer, Heidelberg, Germany), 23–35.

Luo, B., and Minnett, P. J. (2020). Evaluation of the ERA5 sea surface skin temperature with remotely-sensed shipborne marine-atmospheric emitted radiance interferometer data. *Remote Sens.* 12, 1873. doi: 10.3390/rs12111873

Mann, D. G., and Vanormelingen, P. (2013). An inordinate fondness? The number, distributions, and origins of diatom species. *J. Eukaryot Microbiol.* 60, 414–420. doi: 10.1111/jeu.12047

Martinez, E., Antoine, D., D'Ortenzio, F., and Gentili, B. (2009). Climate-driven basin-scale decadal oscillations of oceanic phytoplankton. *Science* 326, 1253–1256. doi: 10.1126/science.1177012

Matías, L., Godoy, O., Gómez-Aparicio, L., and Pérez-Ramos, I. M. (2018). An experimental extreme drought reduces the likelihood of species to coexist despite increasing intransitivity in competitive networks. *J. Ecol.* 106, 826–837. doi: 10.1111/1365-2745.12962

McCabe, R. M., Hickey, B. M., Kudela, R. M., Lefebvre, K. A., Adams, N. G., Bill, B. D., et al. (2016). An unprecedented coastwide toxic algal bloom linked to anomalous ocean conditions. *Geophysical Res. Lett.* 43, 10,366–10,376. doi: 10.1002/2016gl070023

McCann, K. S. (2000). The diversity–stability debate. *Nature* 405, 228–233. doi: 10.1038/35012234

McKibben, S. M., Peterson, W., Wood, A. M., Trainer, V. L., Hunter, M., and White, A. E. (2017). Climatic regulation of the neurotoxin domoic acid. *Proc. Natl. Acad. Sci. U.S.A.* 114, 239–244. doi: 10.1073/pnas.1606798114

Miller, A. J., Chai, F., Chiba, S., Moisan, J. R., and Neilson, D. J. (2004). Decadal-scale climate and ecosystem interactions in the north pacific ocean. *J. Oceanography* 60, 163–188. doi: 10.1023/b:joce.0000038325.36306.95

Millette, N. C., Gast, R. J., Luo, J. Y., Moeller, H. V., Stamieszkin, K., Andersen, K. H., et al. (2023). Mixoplankton and mixotrophy: future research priorities. *J. Plankton Res.* 45, 576–596. doi: 10.1093/plankt/fbad020

Mitra, A., Caron, D. A., Faure, E., Flynn, K. J., Leles, S. G., Hansen, P. J., et al. (2023). The Mixoplankton Database (MDB): Diversity of photo-phago-trophic plankton in form, function, and distribution across the global ocean. *J. Eukaryotic Microbiol.* 70, e12972. doi: 10.1111/jeu.12972

Mitra, A., and Leles, S. G. (2023). "A revised interpretation of marine primary productivity in the Indian ocean: the role of mixoplankton," in *Dynamics of planktonic primary productivity in the Indian ocean*. Eds. S. C. Tripathy and A. Singh (Springer International Publishing, Cham), 101–128.

Montecino, V., Strub, P. T., Chavez, F., Thomas, A., Tarazona, J., Baumgartner, T., et al. (2006). "Chapter 10, Bio-physical interactions off western South America," in *The coastal ocean: interdisciplinary regional studies and synthesis*, vol. 14A . Ed. A. R. Robinson (Harvard University Press, Cambridge), 329–390.

Monteiro, P. M. S., Dewitte, B., Scranton, M. I., Paulmier, A., and van der Plas, A. (2011). The role of open ocean boundary forcing on seasonal to decadal-scale variability and long-term change of natural shelf hypoxia. *Environ. Res. Lett.* 6), 025002. doi: 10.1088/1748-9326/6/2/025002

Montero, P., Daneri, G., Cuevas, L. A., González, H. E., Jacob, B., Lizárraga, L., et al. (2007). Productivity cycles in the coastal upwelling area off Concepción: the importance of diatoms and bacterioplankton in the organic carbon flux. *Prog. Oceanography* 75, 518–530. doi: 10.1016/j.pocean.2007.08.013

Moraga-Opazo, J., Valle-Levinson, A., Ramos, M., and Pizarro-Koch, M. (2011). Upwelling-triggered near-geostrophic recirculation in an equatorward facing embayment. *Continental Shelf Res.* 31, 1991–1999. doi: 10.1016/j.csr.2011.10.002

Nohe, A., Goffin, A., Tyberghein, L., Lagring, R., De Cauwer, K., Vyverman, W., et al. (2020). Marked changes in diatom and dinoflagellate biomass, composition and seasonality in the Belgian Part of the North Sea between the 1970s and 2000s. *Sci. Total Environ.* 716, 136316. doi: 10.1016/j.scitotenv.2019.136316

Olli, K., Ptacnik, R., Andersen, T., Trikk, O., Klais, R., Lehtinen, S., et al. (2014). Against the tide: Recent diversity increase enhances resource use in a coastal ecosystem. *Limnology Oceanography* 59, 267–274. doi: 10.4319/lo.2014.59.1.0267

Osman, M. B., Das, S. B., Trusel, L. D., Evans, M. J., Fischer, H., Grieman, M. M., et al. (2019). Industrial-era decline in subarctic Atlantic productivity. *Nature* 569, 551–555. doi: 10.1038/s41586-019-1181-8

Otero, J., Álvarez-Salgado, X. A., and Bode, A. (2020). Phytoplankton diversity effect on ecosystem functioning in a coastal upwelling system. *Front. Mar. Sci.* 7. doi: 10.3389/fmars.2020.592255

Oyarzún, D., and Brierley, C. M. (2018). The future of coastal upwelling in the Humboldt current from model projections. *Clim Dyn* 52, 599–615. doi: 10.1007/s00382-018-4158-7

Pettitt, A. N. (1979). A non-parametric approach to the change-point problem. *Appl. Stat* 28, 126. doi: 10.2307/2346729

Pezza, A. B., Simmonds, I., and Renwick, J. A. (2007). Southern hemisphere cyclones and anticyclones: recent trends and links with decadal variability in the Pacific Ocean. *Intl J. Climatology* 27, 1403–1419. doi: 10.1002/joc.1477

Pickett, M. H., and Paduan, J. D. (2003). Ekman transport and pumping in the California Current based on the U.S. Navy's high-resolution atmospheric model (COAMPS). *J. Geophys. Res.* 108. doi: 10.1029/2003jc001902

Pizarro, O., Shaffer, G., Dewitte, B., and Ramos, M. (2002). Dynamics of seasonal and interannual variability of the Peru-Chile Undercurrent. *Geophys. Res. Lett.* 29, 22–1.

Pizarro-Koch, M., Pizarro, O., Dewitte, B., Montes, I., Paulmier, A., Garçon, V., et al. (2023). On the interpretation of changes in the subtropical oxygen minimum zone volume off Chile during two La Niña event 2001 and 2007). *Front. Mar. Sci.* 10. doi: 10.3389/fmars.2023.1155932

Ptacnik, R., Solimini, A. G., Andersen, T., Tamminen, T., Brettum, P., Lepistö, L., et al. (2008). Diversity predicts stability and resource use efficiency in natural phytoplankton communities. *Proc. Natl. Acad. Sci. U.S.A.* 105, 5134–5138. doi: 10.1073/pnas.0708328105

Racault, M.-F., Sathyendranath, S., Brewin, R. J. W., Raitsos, D. E., Jackson, T., and Platt, T. (2017). Impact of el niño variability on oceanic phytoplankton. *Front. Mar. Sci.* 4. doi: 10.3389/fmars.2017.00133

Rahn, D. A. (2012). Influence of large scale oscillations on upwelling-favorable coastal wind off central Chile. *J. Geophys. Res.* 117. doi: 10.1029/2012jd018016

Ramajo, L., Valladares, M., Astudillo, O., Fernández, C., Rodríguez-Navarro, A. B., Watt-Arévalo, P., et al. (2020). Upwelling intensity modulates the fitness and physiological performance of coastal species: Implications for the aquaculture of the scallop *Argopecten purpuratus* in the Humboldt Current System. *Sci. Total Environ.* 745, 140949. doi: 10.1016/j.scitotenv.2020.140949

Renault, L., Dewitte, B., Falvey, M., Garreaud, R., Echevin, V., and Bonjean, F. (2009). Impact of atmospheric coastal jet off central Chile on sea surface temperature from satellite observations (2000-2007). *J. Geophys. Res.* 114. doi: 10.1029/2008jc005083

Renault, L., Dewitte, B., Marchesiello, P., Illig, S., Echevin, V., Cambon, G., et al. (2012). Upwelling response to atmospheric coastal jets off central Chile: A modeling study of the October 2000 event. *J. Geophys. Res.* 117. doi: 10.1029/2011jc007446

Rhodes, L. L., Holland, P. T., Adamson, J. E., McNabb, P., and Selwood, A. I. (2003). Production of a new isomer of domoic acid by New Zealand isolates of the diatom *Pseudo-nitzschia australis*. *Molluscan Shellfish Saf.*, 43–48.

Rutllant, J. A., Masotti, I., Calderón, J., and Vega, S. A. (2004). A comparison of spring coastal upwelling off central Chile at the extremes of the 1996–1997 ENSO cycle. *Continental Shelf Res.* 24, 773–787. doi: 10.1016/j.csr.2004.02.005

Ruzicka, J. J., Brink, K. H., Gifford, D. J., and Bahr, F. (2016). A physically coupled end-to-end model platform for coastal ecosystems: Simulating the effects of climate change and changing upwelling characteristics on the Northern California Current ecosystem. *Ecological Modelling.* 331, 86–99. doi: 10.1016/j.ecolmodel.2016.01.018

Sala, O. F., Lauenroth, W. K., McNaughton, S. J., Rusch, G., and Zhang, X. (1996). "Biodiversity and ecosystem function in grasslands," in *Functional role of biodiversity: a global perspective*. Eds. H. A. Mooney, J. H. Cushman, E. Medina and O. E. Sala y ED Schulze (John Wiley & Sons, Nueva York, Chichester, UK), 129–150.

Sauvey, A., Claquin, P., Le Roy, B., Jolly, O., and Fauchot, J. (2023). Physiological conditions favorable to domoic acid production by three *Pseudo-nitzschia* species. *J. Exp. Mar. Biol. Ecol.* 559, 151851. doi: 10.1016/j.jembe.2022.151851

Schneider, W., Donoso, D., Garcés-Vargas, J., and Escribano, R. (2017). Water-column cooling and sea surface salinity increase in the upwelling region off central-south Chile driven by a poleward displacement of the South Pacific High. *Prog. Oceanography* 151, 38–48. doi: 10.1016/j.pocean.2016.11.004

SERNAPESCA (Servicio Nacional de Pesca y Acuicultura). (2022). *Anuario 2017 - Subsector Acuicultura - Statistical Year book 2022 -Aquaculture*. Available online at: http://www.sernapesca.cl/sites/default/files/2017_desembarque_total_region_1.xls.

Shaffer, G., Hormazabal, S., Pizarro, O., and Salinas, S. (1999). Seasonal and interannual variability of currents and temperature off central Chile. *J. Geophys. Res.* 104, 29951–29961. doi: 10.1029/1999jc900253

Shannon, C. E., and Weaver, W. (1949). *The mathematical theory of communication* (Urbana, IL: University of Illinois).

Simpson, E. H. (1949). Measurement of diversity. *Nature* 163, 688–688. doi: 10.1038/163688a0

Smith, R. L. (1968). *Upwelling, oceanographic and marine biology, an annual review* Vol. 6 (London: Allen, and Unwin), pp.11e46.

Stoecker, D. K., Michaels, A. E., and Davis, L. H. (1987). Large proportion of marine planktonic ciliates found to contain functional chloroplasts. *Nature Lond.* 326, 790–792. doi: 10.1038/326790a0

Stone, H. B., Banas, N. S., MacCready, P., Kudela, R. M., and Ovall, B. (2020). Linking chlorophyll concentration and wind patterns using satellite data in the central and northern california current system. *Front. Mar. Sci.* 7. doi: 10.3389/fmars.2020.551562

Takahashi, K., Montecinos, A., Goubanova, K., and Dewitte, B. (2011). ENSO regimes: Reinterpreting the canonical and Modoki El Niño. *Geophys. Res. Lett.* 38. doi: 10.1029/2011gl047364. n/a-n/a.

Tapia, F. J., Navarrete, S. A., Castillo, M., Menge, B. A., Castilla, J. C., Largier, J., et al. (2009). Thermal indices of upwelling effects on inner-shelf habitats. *Prog. Oceanography* 83, 278–287. doi: 10.1016/j.pocean.2009.07.035

Thiel, M., Macaya, E. C., Acuna, E., Arntz, W. E., Bastias, H., Brokordt, K., et al. (2007). The Humboldt current system of northern and central Chile. Oceanographic processes, ecological interactions and socioeconomic feedback. *Oceanogr Mar. Biol. Annu. Rev.* 45, 195–344. doi: 10.1201/9781420050943

Thomas, A. C., Carr, M. E., and Strub, P. T. (2001). Chlorophyll variability in eastern boundary currents. *Geophysical Res. Lett.* 28, 3421–3424. doi: 10.1029/2001GL013368

Tilman, D. (1999). The ecological consequences of changes in biodiversity: a search for general principles. *Ecology* 80, 1455–1474. doi: 10.1890/0012-9658(1999)080[1455:tecoci]2.0.co;2

Tilman, D., Isbell, F., and Cowles, J. M. (2014). Biodiversity and ecosystem functioning. *Annu. Rev. Ecol. Evol. Syst.* 45, 471–493. doi: 10.1146/annurev-ecolsys-120213-091917

Tornquist, F., Bigg, G. R., and Bryant, R. G. (2024). Physical mechanisms affecting phytoplankton variability along the Chilean coast. *J. Mar. Syst.* 242, 103934. doi: 10.1016/j.jmarsys.2023.103934

Toseland, A. D. S. J., Daines, S. J., Clark, J. R., Kirkham, A., Strauss, J., Uhlig, C., et al. (2013). The impact of temperature on marine phytoplankton resource allocation and metabolism. *Nat. Clim Change* 3, 979–984. doi: 10.1038/nclimate1989

Trainer, V. L., Bates, S. S., Lundholm, N., Thessen, A. E., Cochlan, W. P., Adams, N. G., et al. (2012). *Pseudo-nitzschia* physiological ecology, phylogeny, toxicity, monitoring and impacts on ecosystem health. *Harmful Algae* 14, 271–300. doi: 10.1016/j.hal.2011.10.025

Trainer, V. L., Kudela, R. M., Hunter, M. V., Adams, N. G., and McCabe, R. M. (2020). Climate extreme seeds a new domoic acid hotspot on the US west coast. *Front. Clim.* 2. doi: 10.3389/fclim.2020.571836

Utermöhl, H. (1958). Zur Vervollkommnung der quantitativen Phytoplankton-Methodik. *SIL Commun.* 1953-1996 9, 1–38. doi: 10.1080/05384680.1958.11904091

Von Storch, H., and Zwiers, F. W. (1999). Statistical analysis in climate research. *Cambridge Univ. Press Cambridge* p, 484.

Wilkerson, F. P., Lassiter, A. M., Dugdale, R. C., Marchi, A., and Hogue, V. E. (2006). The phytoplankton bloom response to wind events and upwelled nutrients during the CoOP WEST study. *Deep Sea Res. Part II: Topical Stud. Oceanography* 53, 3023–3048. doi: 10.1016/j.dsr2.2006.07.007

Xue, T., Frenger, I., Oschlies, A., Stock, C. A., Koeve, W., John, J. G., et al. (2022). Mixed layer depth promotes trophic amplification on a seasonal scale. *Geophysical Res. Lett.* 49. doi: 10.1029/2022gl098720

Xue, J., Luo, J., Yuan, C., and Yamagata, T. (2020). Discovery of Chile niño/niña. *Geophysical Res. Lett.* 47. doi: 10.1029/2019gl086468